Journal of the Royal Society of New Zealand
Volume 35, Numbers 1 & 2, March/June, 2005, pp 91–122

Integrated outcrop, drill core, borehole and seismic stratigraphic architecture of a cyclothemic, shallow-marine depositional system, Wanganui Basin, New Zealand

T. R. Naish[1], B. D. Field[1], H. Zhu[1], A. Melhuish[1], R. M. Carter[2], S. T. Abbott[3], S. Edwards[2], B. V. Alloway[1], G. S. Wilson[4], F. Niessen[5], A. Barker[6], G. H Browne[1], and G. Maslen[1]

Abstract Late Pliocene to mid-Pleistocene (c. 2.1–0.4 Ma) strata exposed in the, now classical, Nukumaru and Castlecliff coastal cliff sections north-west of Wanganui comprise 25, 6th (41 ka) order and 5th (100 ka) order, shallow-marine to marginal marine stratigraphic sequences, deposited during global glacio-eustatic sea-level cycles corresponding to Marine Isotope Stages (MIS) 78–10. Here, we characterise the sequences using: (1) a series of drill cores sited above and behind the coastal outcrops, which recovered a composite record of c. 450 m, (2) a new high resolution multichannel seismic reflection profile acquired along the beach adjacent to the coastal cliffs, and (3) downhole digital logs from the boreholes. This paper integrates the outcrop and subsurface datasets to produce a high resolution model of the stratigraphic signatures and 2D architecture of a cyclical, shallow-marine deposition system. Such models have significant applications to petroleum exploration, and enable the distribution of reservoir facies and intervening seal rocks within sequences, together with the nature of the connectivity of sandstone facies between sequences, to be evaluated. Similar hydrocarbon-producing systems within the Eocene Kapuni Group (e.g., Mangahewa and Kaimiro formations) have been, and are still, the focus of intense exploration in Taranaki Basin.

Keywords sequence statigraphy; Wanganui Basin; Pliocene-Pleistocene; shallow-marine; cyclothem; seismic reflection; borehole; drillcore

INTRODUCTION

Continental margins are relatively rare that afford an opportunity to study the stratigraphic architecture of shallow-marine depositional systems on spatial scales ranging from core and borehole (millimetres/centimetres) to outcrop and seismic (tens of metres), during periods of known sea-level oscillations. Wanganui Basin (Fig. 1) is one of a small number of Pliocene-Pleistocene basins worldwide (Kitamura et al. 2000; Browne & Naish 2003) in which sedimentation evidently kept pace with subsidence through much of the basin history, resulting in a 5 km thick record of predominantly shelf and shallow water sediment (Fleming 1953;

[1]Institute of Geological and Nuclear Sciences, P.O. Box 30 368, Lower Hutt, New Zealand. Email: t.naish@gns.cri.nz
[2]Marine Geophysical Laboratory, James Cook University, Townsville, Queensland 4811, Australia.
[3]School of Environmental Science and Management, Southern Cross University, P.O. Box 157, East Lismore, NSW, 2480, Australia.
[4]Department of Geology, University of Otago, P.O. Box 56, Dunedin, New Zealand.
[5]Alfred-Wegener-Institute for Polar and Marine Research, P.O. Box 120161, D-27515 Bremerhaven, Germany.
[6]Department of Earth Sciences, Parks Road, Oxford OX1 3PR, United Kingdom.

R05007 Received 17 April 2005; accepted 31 May 2005; Online publication date 27 July 2005

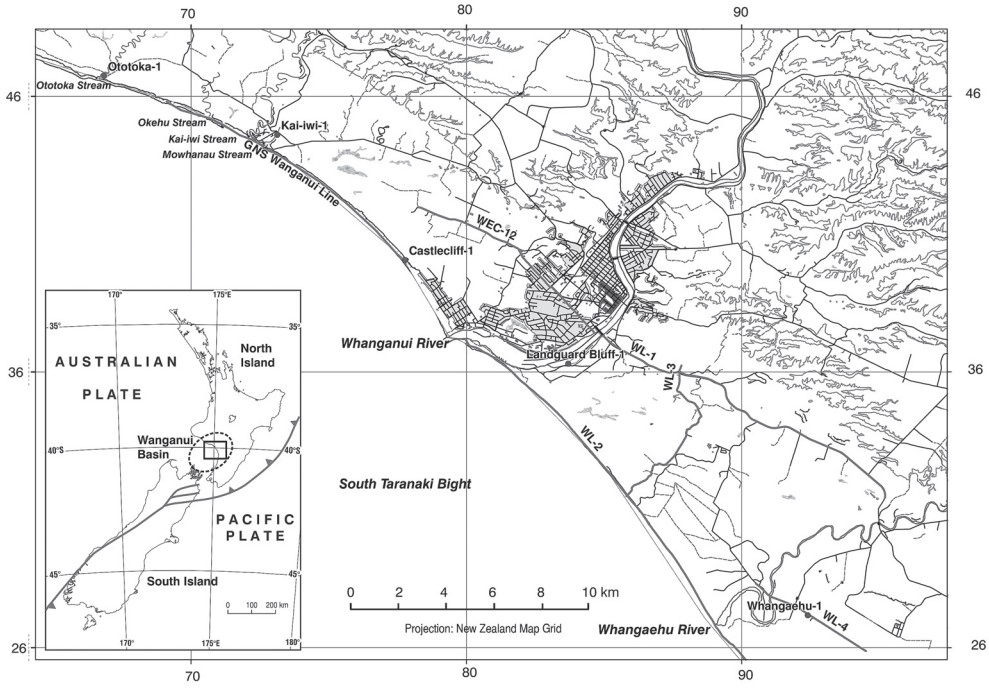

Fig. 1 Location of seismic lines and drill holes used in this study. GNS Wanganui Line is the c. 12 km long, high resolution seismic reflection profile acquired along the beach to the north-west of Wanganui City. Castlecliff-1, Kai-iwi-1, and Ototoka-1 holes were continuously cored behind the coastal outcrop and correlated with the seismic line. Onland industry seismic data (WL and WEC lines) and the Whangaehu-1 exploration well are also shown for reference.

Anderton 1981). Gentle upwarping of the eastern margin of the basin has produced spectacular exposures along coastal cliffs and inland within the heavily dissected and uplifted landscape, through as many as 44 depositional sequences deposited during the last 2.5 Ma (Naish et al. 1998; Carter et al. 1999; Saul et al. 1999).

The Wanganui stratigraphic succession comprises a range of siliciclastic and carbonate sediments deposited in shelf, shoreline, and coastal plain depositional environments during orbitally controlled, sea-level fluctuations of 41 ka and 100 ka duration. Over the last 10 years this margin has gained a reputation as one of the world's outstanding outcrop examples of a Pliocene-Pleistocene shallow-marine, clastic depositional system (e.g., summary papers: Abbott & Carter 1994; Abbott 1997; Naish & Kamp 1997; Kamp & McIntyre 1998; Naish et al. 1998; Saul et al. 1999). Outcrop analogues of this quality are rare, as most Quaternary shelf margins underlie flooded continental shelves (e.g., Gulf of Mexico). While the basin has not yielded any significant hydrocarbon prospects, the Wanganui sequences represent an important exploration outcrop analogue for prospective shallow-marine depositional systems in adjacent Taranaki Basin (e.g., Kapuni Group). The Wanganui sequences also provide a shallow-marine counterpart to the Miocene slope and basin floor sediments that are spectacularly exposed on the north Taranaki coastline (King et al. 1994; Browne et al. 2000).

Here, we present results from a series of drill holes through the shallow-marine sediments of the Nukumaru and Castlecliff sections, exposed in coastal cliffs north-west of Wanganui City (Fig. 1, 2). The drilling recovered a continuous, c. 450 m thick record of sedimentary

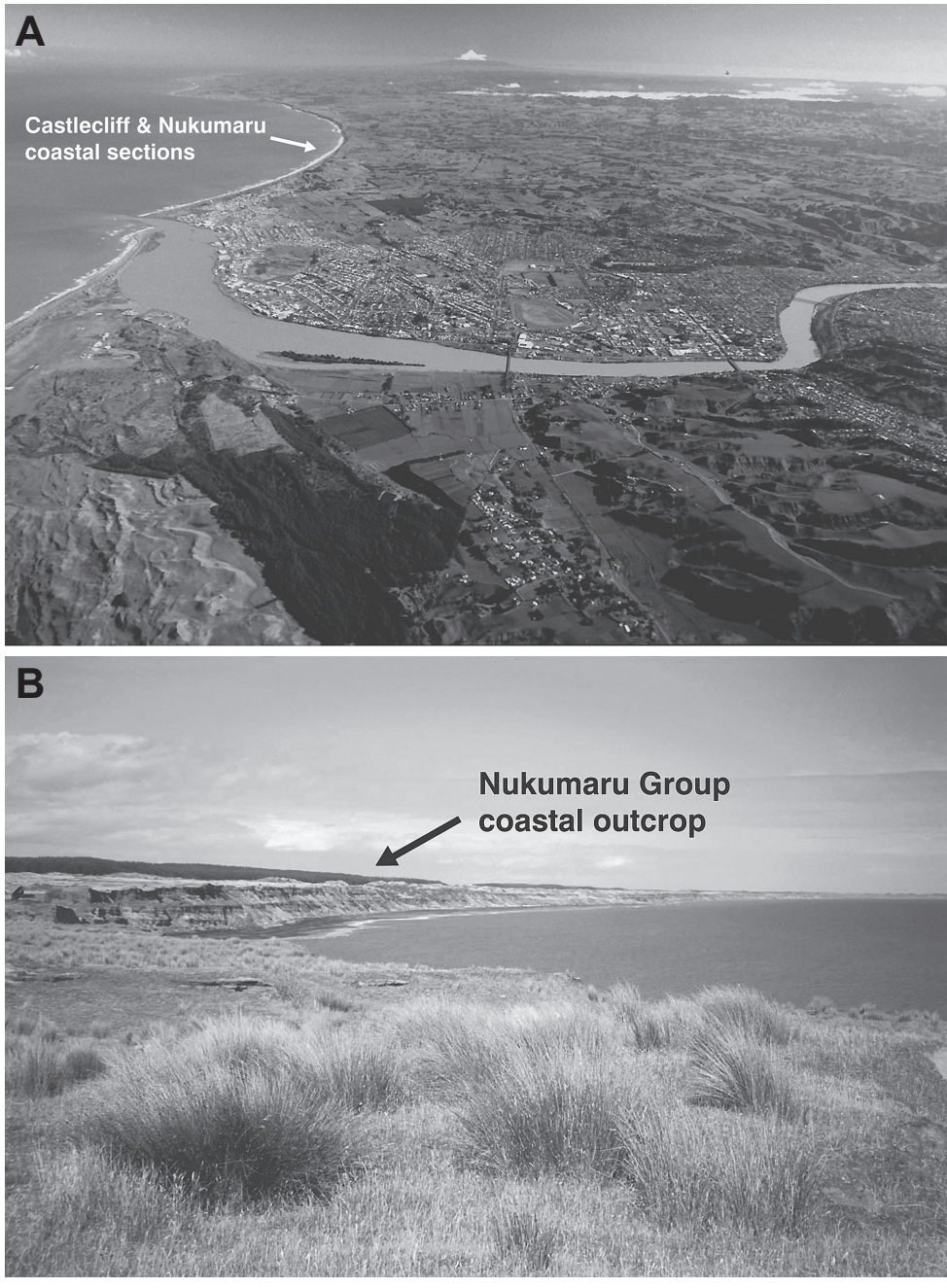

Fig. 2 **A**, Aerial view of the Castlecliff and Nukumaru coast section north-west of Wanganui City. **B**, Nukumaru Group coastal exposures south-east of Waitotara River.

sequences deposited during Marine Isotope Stages (MIS) 78–10 (2.1–0.4 Ma). This paper summarises the integration of the new behind-outcrop drill hole (Fig. 3A) data with both the established outcrop stratigraphy (Fig. 2A) and new below-outcrop seismic reflection profiles

Fig. 3 **A**, Operation during drilling of Castlecliff-1A on the terrace above the outcropping cliff section. **B**, Seismic survey operations near Kai-iwi Beach.

(Fig. 3B), with the aim of improving models for the recognition and interpretation of high frequency shallow-marine depositional sequences. The figures in this paper are summarised from a series of large colour poster charts, which are available in electronic format from

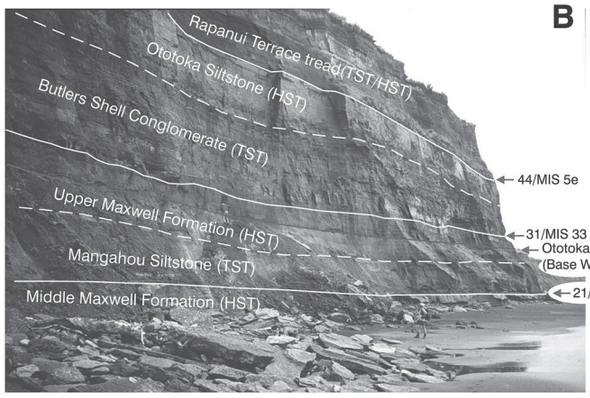

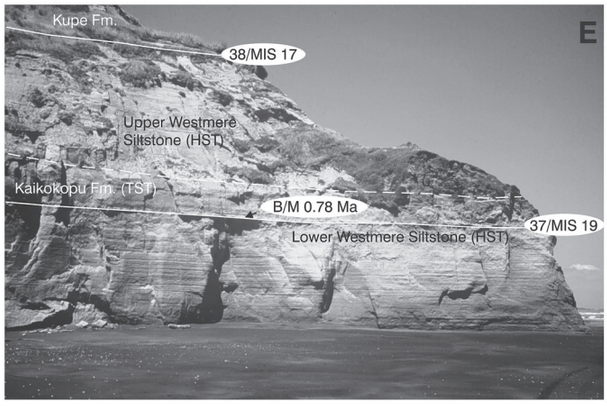

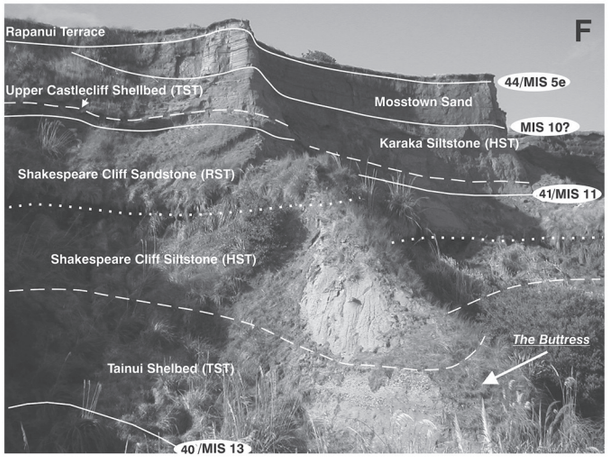

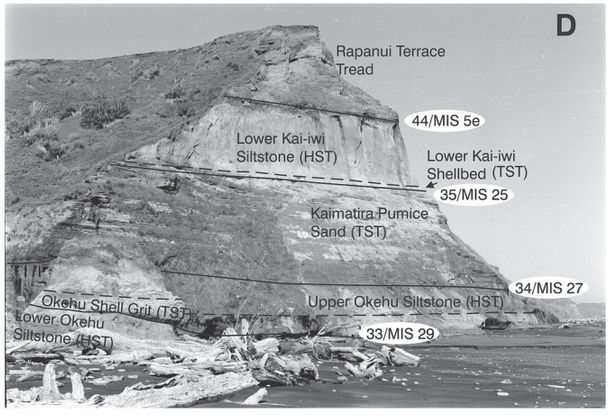

Fig. 4 **A**, Outcropping shallow-marine sequences of the Nukumaru Group at Nukumaru Beach. **B**, Formations and marginal-marine sequences near the top of the Nukumaru Group, below the Butlers Shell Conglomerate. Shown is the location of the Ototoka Tephra, which at this location marks the section stratotype and point for the base of the Castlecliffian Stage. Note that c. 450 ka (MIS 56–34), equivalent to basin cycles 32–22, is locally missing at the unconformity at the base of the Butlers Shell Conglomerate. **C**, Locally, at Ototoka Stream, the unconformity at the base of the Butlers Shell Conglomerate occurs as a large channel incised into the Mangahou Siltstone, and infilled with a shallow water trough-cross-bedded shelly conglomerate (TST of basin cycle 31). Ototoka-1 was drilled on the Rapanui Terrace to the right of the photo. **D**, Bluff on the south side of Okehu Stream contains spectacular exposures through basin cycles 33 and 35. The TST of cycle 34 (Kaimatira Pumice Sand) is over-thickened by the rapid introduction of volcaniclastic sediment associated with the Potaka Tephra eruption from the Taupo Volcanic Zone c. 1 Ma. Sequence boundary at the base of cycle 35 (MIS 25) truncates the HST and RST of the underlying sequence, which are preserved basinward of the outcrop in the high resolution seismic line. **E**, Coastal outcrop sequence stratigraphy exposed in the Castlecliff section in the vicinity of the Lower-Middle Pleistocene Boundary. The Matuyama-Brunhes palaeomagnetic boundary (0.78 Ma) occurs in the sequence boundary at the base of the Kaikokopu Shellbed (basin cycle 37; MIS 19). Kupe Formation in the TST of the overlying basin cycle 38 contains the Kupe Tephra. **F**, Sequences (cycles 40 and 41; MIS 13–11) of the upper part of the Shakespeare Group exposed at the southeastern end of the Castlecliff section in "The Buttress". Here the fossiliferous Tainui Shellbed (TST of basin cycle 40) is spectacularly exposed. Cycle 40 is one of the few cases where the highstand shelf to regressive shoreline facies (forced regressive) assemblage is preserved as the Shakespeare Cliff Siltstone and Sandstone.

www.gns.cri.nz. We offer this integrated package, which utilises a range of industry standard geological datasets (e.g., wireline electric logs, formation microresistivity image logs, core sedimentary facies analysis, and seismic reflection profiles), as a basis for training courses and workshops.

OUTCROP STRATIGRAPHY

Nukumaruan coastal stratigraphy

A c. 250 m thick succession of Late Pliocene to early Pleistocene (c. 2.4–1.63 Ma) strata exposed in coastal cliffs south of the Waitotara River mouth and along Nukumaru and Ototoka beaches, between the Kuranui Limestone and the base of the Butlers Shell Conglomerate, has traditionally comprised the "type formations" of the Nukumaruan Stage in New Zealand (Fleming 1953) (Fig. 1, 2). The Nukumaruan strata are exposed in the lower parts of the cliffs, and dip gently towards the south (Fig. 4). The upper parts of the cliffs comprise flat-lying Late Pleistocene marine terrace cover (MIS 5e, Rapanui Terrace), that unconformably overlies the Nukumaruan strata. The cliffs are vegetated and fresh exposure is created regularly by mass wasting. Consequently, the degree, location, and quality of exposure vary over time.

Abbott et al. (2005 this issue) describe 11 depositional sequences through the well exposed upper 86 m of the Nukumaruan coastal section above the Nukumaru Limestone, which comprise Nukumaru Brown Sand, Tewkesbury Formation, Lower Maxwell Formation, Pukekiwi Shell Sand, Middle Maxwell Formation, Mangahou Siltstone, and Upper Maxwell Formation (Fig. 4, 5). These sequences consist predominantly of siliciclastic shoreline facies. Non-marine facies (including palaeosols), and a variety of shallow-marine shellbed facies, are also represented. The sequences are characterised by repetitive vertical facies successions that represent deposition in a shallow-marine shoreline and inner shelf to swampy coastal plain setting during the rise, highstand, and early fall of 41 ka duration glacio-eustatic sea-level cycles. The older formations of the Nukumaru Group, exposed along the coast immediately south-east of the Waitotara River mouth are not so well exposed in coastal cliffs. Fleming (1953) identified four cycles of shallow water coquina limestone and well sorted sandstone. Drill core and borehole records in this study recovered Nukumaruan strata spanning the top of the Nukumaruan Limestone to the base of the Butlers Shell Conglomerate, and are equivalent to the 11 sequences (Wanganui Basin cycles 11–21) correlated with MIS 78–57 by Abbott et al. (2005 this issue) (Fig. 5).

Recently, Beu et al. (2004) redefined the boundary between the Nukumaruan (Wn) and Castlecliffian (Wc) stages at the level of the base of the Ototoka Tephra, several metres below the Butlers Shell Conglomerate (Fig. 4B), and assigned it an age of 1.63 Ma based on fission track chronology and astronomical calibration. The new section stratotype and point is at Ototoka Beach (Fig. 4). This has removed the stratigraphic ambiguity associated with the historical placement of the base of the Wc in the local unconformity (at the base of the Butlers Shell Conglomerate) spanning some 450 ka. Consequently, Wanganui Basin cycles 22–30, which correspond to MIS 56–34, and are recognised elsewhere in the Basin, are now ascribed to the Castlecliffian Stage (see Pillans et al. 2005, this issue).

Castlecliffian coastal stratigraphy

The immediately overlying, 160 m thick Castlecliff coast section was deposited during the Middle Pleistocene (c. 1.07–0.35 Ma) and comprises 10 unconformity-bound cyclothems, or sequences, described by Abbott & Carter (1994, 1998) (Fig. 4, 5). This "classical" outcrop section comprises the "type" groups and formations of the Castlelcliffian Stage (Fleming 1953). Its cyclical, shallow-marine facies contain extant molluscan fossil associations that allowed

recognition by Fleming (1953) of 10 oscillations in relative sea level from shelf to shoreface water depths. The sequences comprise facies stacked in repetitive vertical successions consisting predominantly of shallow-marine transgressive fossiliferous sandstones and mudstones, offshore shelfal shellbeds, and in some cases regressive shelf to shoreface assemblages deposited during the rise, highstand, and early fall of a cycle of relative sea level.

More recent sequence stratigraphic and chronostratigraphic studies of the strata (described below) have allowed the identification of six, 6th order sequences deposited during 41 ka duration sea-level cycles associated with MIS stages 31–20, and four, 5th order sequences deposited during 100 ka duration sea-level cycles associated with MIS stages 19–10 (Abbott & Carter 1994; Pillans et al. 1994; Naish et al. 1998; Saul et al. 1999).

Facies architecture and sequence stratigraphy

Sequence stratigraphic studies of the Pliocene-Pleistocene sediments within Wanganui Basin have utilised the recognition of vertically stacked, cyclic facies successions, bounded by sharp erosional surfaces that mark prominent lithologic dislocations, as the basis for identifying depositional sequences. Facies and biofacies analyses allow interpretation of the spatial and temporal pattern of environmental change within sequences. Accurate interpretation of sequence architecture is greatly aided by an understanding of shellbed types present (e.g., summarised in Naish et al. 2005b this issue, table 2), and the habitat of their faunas, as first appreciated by Fleming (1953). The taphonomic features of the shellbeds have allowed intervals of stratigraphic condensation due to marine reworking by waves and currents, sedimentary bypassing, or non-deposition, to be identified. Thus, the recognition of (1) vertically stacked facies successions bounded by sharp erosion surfaces (sequence boundaries), together with (2) the distinctive shellbeds and their associated stratal discontinuities, delineate the stratigraphic geometry of the sequences and allow systems tracts to be differentiated (e.g., *sensu* Vail 1987). The scheme used here to describe and interpret sedimentary facies in the outcrop sections and drill core draws on previous studies by Abbott & Carter (1994), Naish & Kamp (1997), and Abbott et al. (2005 this volume), and is summarised in Table 1.

Naish & Kamp (1997) and Kondo et al. (1998), after Kidwell (1991), have recognised onlap, backlap, downlap, and flooding surface shellbeds. These shellbeds are associated, respectively, with the transgressive surface of erosion, a local flooding surface, the downlap surface, and paracycle-bounding marine flooding surfaces. In offshore settings, where the downlap surface converges with the sequence boundary, elements of both onlap and downlap shellbeds may become superposed. For such cases the term "compound shellbed" is useful. Abbott & Carter (1994) distinguished type A shellbeds within the transgressive systems tract (reworked shallow water species, often cross-bedded); and type B shellbeds (offshore shelf species, preserved *in* or *near situ*), which straddle the junction between the transgressive and highstand systems tracts, leading to the term "mid-cycle shellbed".

Abbott & Carter (1994) and Abbott et al. (2005 this issue) applied a sequence stratigraphic model to subdivide the mid-Pleistocene Castlecliff section and Late Pliocene-Pleistocene Nukumaru section sediments, respectively, into stratigraphic sequences representing cycles of relative sea-level change. Twenty depositional sequences have been identified (Fig. 5). Each sequence typically contains the following architectural elements in ascending stratigraphic order. Figure 6 illustrates the conceptual sequence stratigraphic model.

1. A basal sequence boundary (SB) consisting of an unconformity, which is coincident with the transgressive surface of erosion (TSE) (Fig. 6).
2. A transgressive systems tract (TST), corresponding mainly to a condensed fossiliferous deepening upwards interval comprising shellbed facies Cz1 and/or Cs1. Commonly an onlap shellbed containing shallow water infaunal molluscs (sandy Cs1 and sometimes reworked

Cs2) is overlain by a backlap shellbed (Cz2), comprising significantly more *in situ* epifaunal components (molluscs, barnacles, brachiopods, and bryozoans) within a siltstone matrix of offshore shelf affinity. These superposed, or vertically gradational, shellbed units are termed "compound shellbeds". Onlap shellbeds may be overlain by sand rich shoreline facies (S5 and S11), or heterolithic laminated and bedded intertidal facies (S7, Z8).
3. A downlap surface (DLS).
4. A highstand systems tract (HST) comprising an aggradational interval of bioturbated shelf siltstone (Z_1–Z_3), or sandier shoreline innershelf facies (S1–S3), depending on position on the palaeoshelf.
5. A regressive systems tract (RST) that marks a transition from fine sandy siltstone (Z4) or fine sandstone facies (S4) of inner shelf affinity in the upper HST to strongly progradational, "forced" regressive shoreface-foreshore-intertidal facies assemblage (S5–8). In some Nukumaruan sequences marginal marine swamp/lacustrine (S10, Z7, Z5) and coastal plain (Z6, S9) facies are preserved in the top of RSTs below the sequence boundary.

Wanganui Sequence motifs

Saul et al. (1999) recognised six distinctive styles of sequence architecture that they termed "motifs". Recent work in the eastern portion of the basin (Naish & Pillans unpubl. data), and a redescription of the Nukumaruan stratotype section (Abbott et al. 2005 this issue) have led to the recognition of five new motifs. Figure 6 outlines the characteristics of 11 distinct styles of sequence motif recognised in Wanganui Basin, and places them within an idealised 2D sequence stratigraphic model. Faunal, sedimentological, and stratigraphic evidence indicates that the sequence types described below represent successively more offshore locations on the palaeoshelves that equate with each sequence. The fluvial, lacustrine, swampy lignitic, and shallow-marine facies within the Birdgrove, Oroua, and Pakihikura motifs correspond to coastal plain and paralic environments. Adjacent to the same shoreline, but on the gradually emerging western flank of the basin, the coquina-dominated Nukumaru motif and the sediment-starved Maxwell motif, also represent shallow water environments. Offshore on the inner to middle shelf, Tewkesbury, Castlecliff, and Seafield sequence motifs are characteristic. Farthest offshore, toward the basin axis, Rangitikei motif sequences were deposited, mostly inboard of the lowstand shoreline in outer shelf depths of 60 m or greater.

Chronology of the outcropping strata

An integrated chronology for the outcropping Nukumaruan-Castlecliffian strata has been developed based on radiometric ages on interbedded rhyolitic tephra (Alloway et al. 1993; Pillans et al. 1994; Pillans et al. 2005 this issue), on biostatigraphic data (Beu & Edwards 1984), on palaeomagnetic polarity measurements (Turner & Kamp 1990; Pillans et al. 1994), and on cycle correlations with the oxygen isotope timescale (Abbott & Carter 1994; Pillans et al. 1994; Naish et al. 1998). Key chronostratigraphic datums include:
1. Ototoka Tephra in basin cycle 21, which has an isothermal plateau fission track (ITPFT) age of 1.71 ± 0.19 Ma, and is correlated with MIS 57.
2. Base Jaramillo Subchron, which is correlated with MIS 31 in deep sea cores (Shackleton et al. 1990), which occurs in the Ototoka Siltstone in basin cycle 31.
3. Top Jaramillo Subchron, which is correlated with MIS 27 in deep sea cores (Shackleton et al. 1990), and occurs at the top of the Kaimatira Pumice Sand in basin cycle 34.
4. Reworked Potaka Tephra Kaimatira Pumice Sand in basin cycle 34, which has an ITPFT age of 1.05 ± 0.05 Ma, and is correlated with MIS 27.
5. Reworked Kaukatea Tephra in basin cycle 35, which has an ITPFT age of 0.86 ± 0.08 Ma, and is correlated with MIS 25/23.

6. Matuyama/Brunhes Boundary, which is correlated with the MIS 20/19 transition in deep sea cores (Shackleton et al. 1990), and occurs in the unconformity at the base of the Kaikokopu Shellbed (basin cycle 37).
7. The first appearance of the *Pecten* during MIS 19 in the Upper Westmere Shellbed.
8. Kupe Tephra in basin cycle 38, which has an ITPFT age of 0.63 ± 0.08 Ma, and is correlated with MIS 19.

Numeric ages on the tephra are consistent with both the interpreted magnetostratigraphy and cyclostratigraphy, and fit well with the astronomically calibrated timescale. The cycle correlations provide age estimates for the development of lowstand unconformities, transgressive surfaces of erosion, and intervals of maximum water depth within sequences, thereby allowing sequence and facies development to be evaluated in terms of known phases of global sea-level change.

DRILL CORE STRATIGRAPHY

Drill cores were recovered from three stratigraphic holes sited on the Rapanui Terrace (MIS 5e) above and behind the coastal outcrops (Fig. 1). The holes were offset along the coast to intersect the entire 2–3°, southward dipping stratigraphic succession between the top of the Nukumaru Limestone (MIS 79) to the Karaka Siltstone (MIS 11). Drilling was undertaken in September 1999, by Drillwell Exploration Ltd, using a minerals industry, truck-mounted drill rig with a wireline rotary diamond coring system. A continuous PQ (c. 100 mm) and HQ (c. 60 mm) core was recovered by tripping core barrels of 2 and 3 m length out of the hole. Core recovery ranged from 98% for Castlecliff-1 to 60% in the much sandier Ototoka-1 borehole. Recovery of well sorted unconsolidated sands proved problematic in both Kai-iwi-1 and Ototoka-1, with significant losses. Moreover, a number of the sandy lithologies (e.g., Nukumaru Brown Sand) produced artesian groundwater flows that proved difficult to control and led to premature abandonment of Kai-iwi-1. Notwithstanding these problems, the three boreholes/drill cores did provide an overlapping composite record of the stratigraphic succession exposed in the Nukumaru and Castlecliff coastal sections. We have not used data from the Landguard Bluff-1 well (Fig. 1), a stratigraphic research well drilled on the south bank of the Whanganui River in the early 1980s, as correlation of the lower part of this well with the upper part of the Castlecliff-1A well is not straightforward. This is because a series of active NW-SE trending normal faults, which underlie the Whanganui Valley and separate the two wells, have resulted in a thicker Late Pleistocene succession on the south side of the river. Preliminary stratigraphic descriptions of the drill cores were made at the drill site. Subsequently, the cores were described in centimetre to millimetre resolution at the Institute of Geological and Nuclear Sciences, as the basis for sedimentary facies analysis and sequence stratigraphic interpretation.

Castlecliff-1A

Castlecliff-1A represents a composite of two drillholes. Castlecliff-1 was spudded in September 1999, 70 m from the edge of the coastal cliff in a new coastal subdivision at the end of Longbeach Drive (R22/777406; Fig. 3D). It was cored continuously to a depth of 192.46 m. Subsequently, a new hole was drilled 5 m away from the original in 2000 for downhole geophysical logging. This hole, Castlecliff-1A, was wash drilled (no core) to 220.15 m. Below 190 m, cuttings were described to extend the composite stratigraphic record to 220 m.

The recovered stratigraphic record (Fig. 7) comprises eight, unconformity-bounded depositional sequences correlated with basin cycles 34–41. Sequence bounding unconformities are typically sharp, planar surfaces, separating bioturbated siltstone from overlying current-bedded

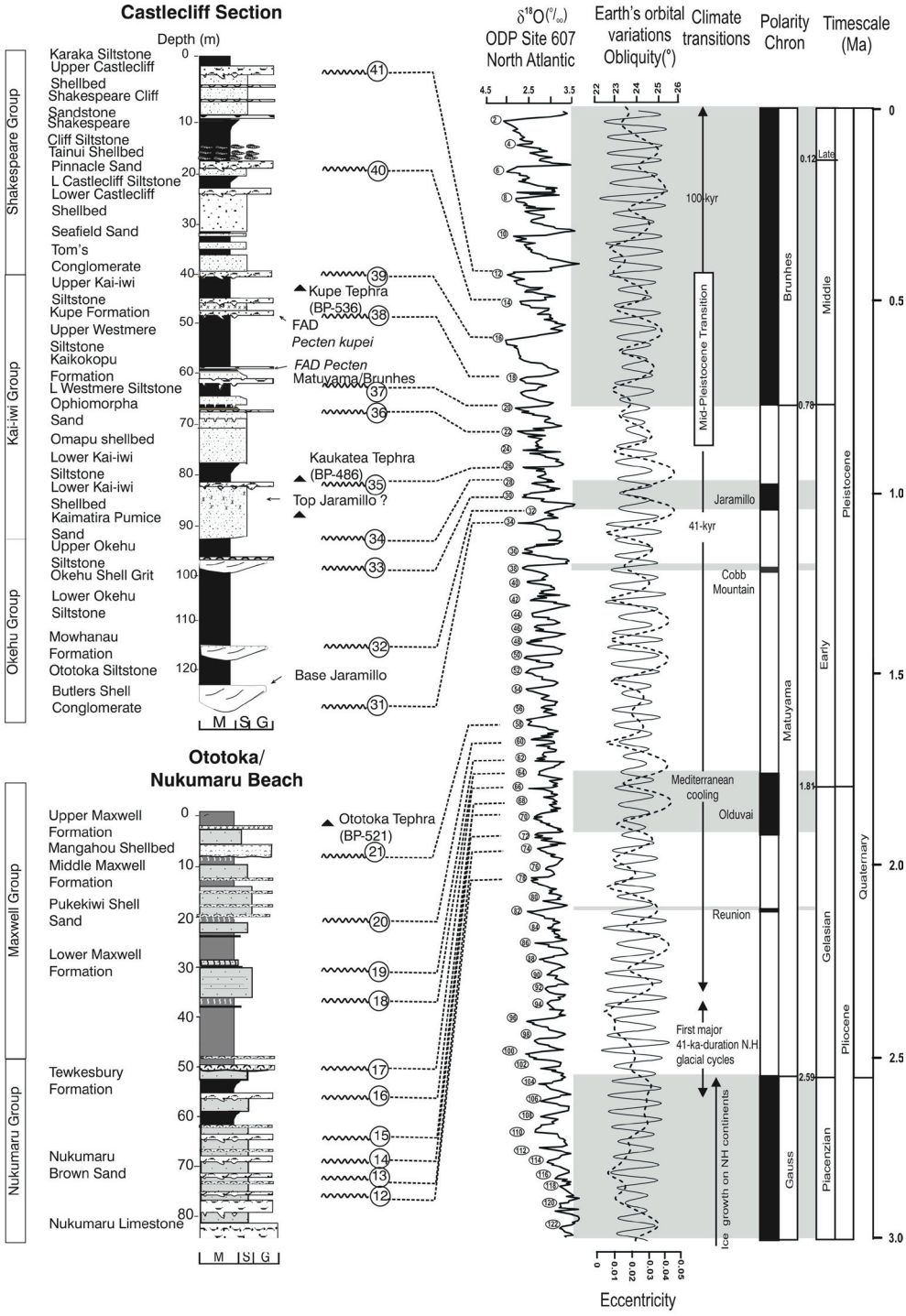

Fig. 5 Composite stratigraphic columns for the Nukumaru and Castlecliff coastal sections showing lithostratigraphy, sequence stratigraphy, and correlations with the oxygen isotope timescale.

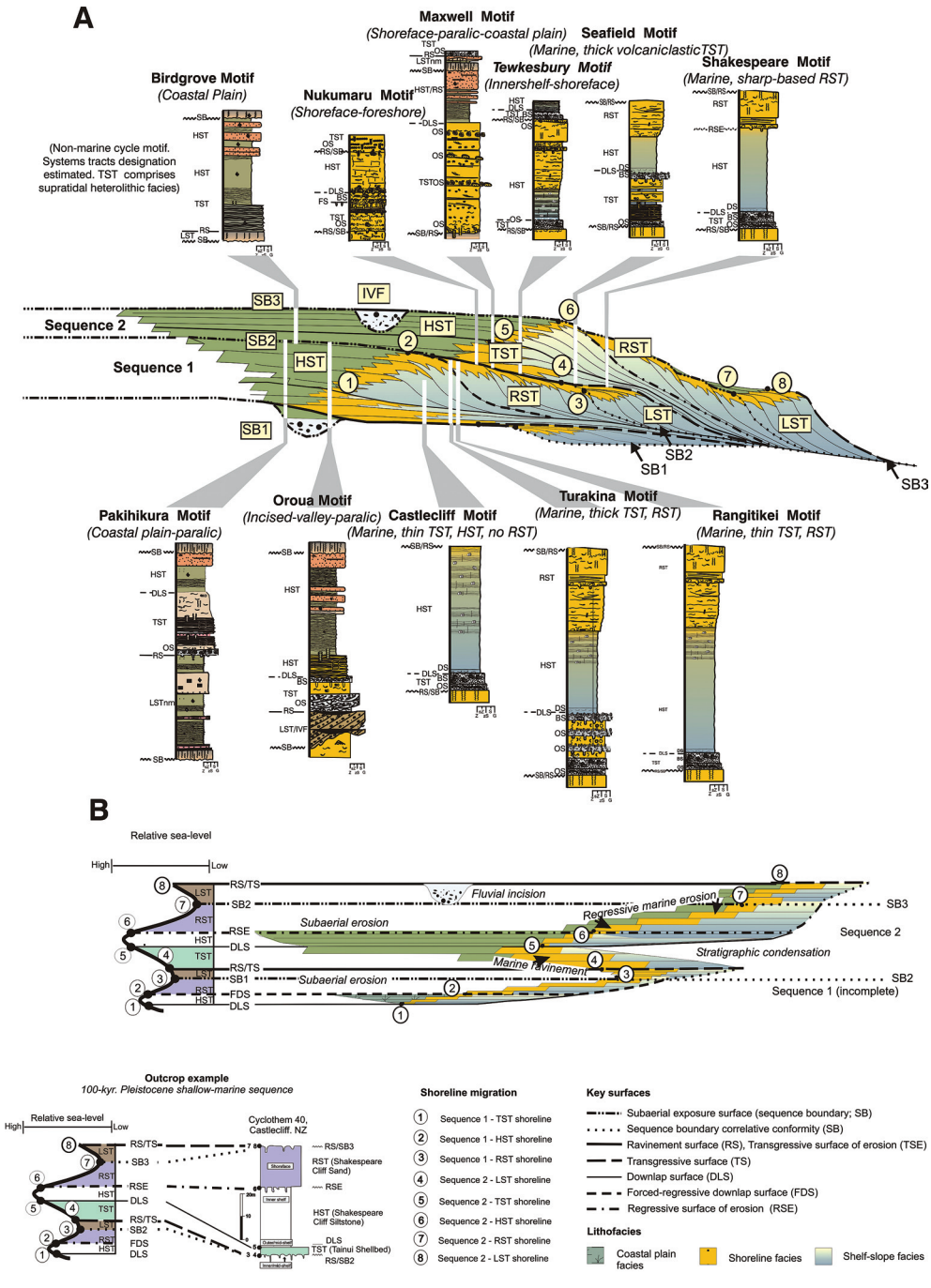

Fig. 6 Conceptual A, sequence stratigraphic and B, chronostratigraphic models for Milankovitch-scale Wanganui Basin depositional sequences. The stratigraphic architecture and timing of development of systems tracts and key surfaces are shown with respect to a relative cycle of sea level. Outcrop motifs of Wanganui sequences are illustrated in the context of a 2D coastal plain to outer shelf progradational setting.

fossiliferous sandstone. The sequences comprise facies stacked in repetitive vertical successions consisting predominantly of shallow-marine transgressive fossiliferous sandstones and mudstones (1–25 m thick), offshore shelfal shellbeds at the mid-cycle position (<1 m thick), an interval of massive to wavy-bedded shelf siltstone (3–25 m thick), and in some cases regressive shelf to shoreface sandstone facies assemblages (2–5 m thick) deposited during the rise, highstand, and early fall of sea level, respectively.

Kai-iwi-1

Kai-iwi-1 was spudded in in September 1999, 750 m inland from the coastal section in the Mowhanau River valley near the intersection of the Mowhanau Village Road and Rapanui Road (R22/732450). It was continuously cored to 105.5 m where the hole was abandoned due to poor core recovery and unstable drilling conditions through several sandstone intervals with artesian groundwater flows. No borehole logging was undertaken on this hole.

The recovered cored interval (Fig. 8) was 80% complete, and comprised nine, unconformity-bounded depositional sequences correlated with basin cycles 23–34. The interval above 68.25 m spanning the Butlers Shell Conglomerate to the Kaimatira Pumice Sand contained four shallow-marine sequences of similar character to those in Castlecliff-1A, and was readily matched to the nearby coastal outcrop stratigraphy (Abbott & Carter 1994). The sedimentary succession below 68.25 m comprised a range of carbonaceous siltstones and sandstones, palaeosols and lignites correlated with the non-marine to marginal marine Maxwell Group. The interval has been subdivided into five unconformity-bound sequences based on the recognition of sharp-based marginal marine shellbeds and palaeosols, and on correlation with the seismic stratigraphy (see below).

Ototoka-1

Ototoka-1 was spudded in October 1999, 200 m inland from the edge of coastal section on the south-east side of Ototoka Stream (R22/669472). It was cored continuously to 123.8 m, where the hole was terminated in the Nukumaru Limestone. This hole also suffered from widespread borehole collapse through aquifers in the Nukumaru Brown Sand, resulting in poor core recovery through the lower 50 m. However, with the use of the formation micro-image (FMI) logs, along with intermittent core allowed a more or less continuous stratigraphy to be described (Fig. 9).

The recovered cored interval was 60% complete and comprises a similar stratigraphy to that of the coastal section described by Abbott et al. (2005 this issue). Nine unconformity-bounded, shallow-marine and marginal-marine to non-marine deposition sequences corresponding to basin cycles 12–21 are described in Fig. 9.

Facies architecture and sequence stratigraphy

The same facies and sequence stratigraphic approaches outlined by Abbott & Carter (1994) and Abbott et al. (2005 this issue), and summarised above were applied to the analysis of the drill core sediments. Facies descriptions and interpretations are summarised in Table 1. Sequence stratigraphic interpretations, together with depositional environments and inferred palaeobathymetric fluctuations, are shown on Fig. 7, 8, and 9 for the three cored intervals. A higher resolution analysis of the core and borehole FMI image in the context of key sequence stratigraphic surfaces and facies at the bed scale is discussed below, and illustrated in Fig. 10–12. The composite stratigraphic record comprises 25, shallow-marine to non-marine, orbitally controlled 5th (100 ka) and 6th (41 ka) order depositional sequences deposited during glacio-eustatic sea-level cycles of 30–120 m amplitude (MIS 78–10).

Chronology of the drill core sediments

Palaeomagnetism

One hundred-and-seventy-one oriented samples (with respect to vertical) were taken from drill cores from the three holes for palaeomagnetic analysis. Magnetic measurements were made on a CCL cryogenic magnetometer in a low field environment at Oxford University (Barker 2001). All samples were subject to stepwise thermal demagnetisation in steps of 20°C up to 100°C, followed by stepwise alternating field demagnetisation in steps of 5 mT increments. Magnetic susceptibility measurements were made to monitor mineralogy changes.

Two main interpretative methods were used to identify characteristic site remanence directions. Where possible, linear trends were isolated for discrete samples from orthogonal vector component plots using a free line fit (Butler 1992). Where it was not possible to identify characteristic remanence directions because samples contained more than one component of magnetisation, site directions were identified using remagnetisation great circle analysis on stereographic projections of demagnetisation data. The treatment and interpretation of data are dealt with in more detail in Barker (2001) and Wilson et al. ("A revised paleomagentic stratigraphy for Plio-Pleistocene, shallow-marine cyclothems, Castlecliff and Nukumaru coastal sections, Wanganui Basin, New Zealand" in prep.).

The quality of the data enabled an N-R-N (upward) polarity zonation to be established for the Castlecliff-1A core, which is consistent with the previously published magnetostratigraphy for the Castlecliff outcrop section (Turner & Kamp 1990) (Fig. 13). Polarity transitions occurring at 180 m and 135.36 m confirm the identification of the top of the Jaramillo Subchron (0.99 Ma, MIS 27) in the Lower Kai-iwi Shellbed and the Matuyama-Brunhes Boundary at the base of the Kaikokopu Shellbed (0.78 Ma, MIS 20/19), respectively. The normal interval below 180 m comprises reworked Potaka Tephra (1.05 ± 0.05 Ma) within the Kaimatira Pumice Sand, which is consistent with the occurrence of the Potaka Tephra in the Jaramillo Subchron elsewhere in Wanganui Basin (Pillans et al. 1994, 2005 this issue).

An R-N (upward) polarity zonation for the Kai-iwi-1 core is stratigraphically incomplete due to substantial core losses between 110–95 m and 90–65 m, but is consistent with the known position of the base of the Jaramillo Subchron (1.07 Ma; MIS 31) in the Ototoka Siltstone in the Castlecliff outcrop section (Turner & Kamp 1990) (Fig. 13). The polarity transition in Kai-iwi-1 is poorly defined but occurs between 80 and 60 m.

An N-R (upward) polarity zonation is established for the Ototoka-1 core, which, based on a limited number of samples, is tentatively correlated with the top of Olduvai Subchron (Fig. 13). The transition at c. 50 m occurs within the non-marine Lower Maxwell Formation at the base of basin cycle 18, and is consistent with the identification of the top of the Olduvai Subchron (1.79 Ma; MIS 63) in the Rangitikei Valley at the base of cycle 18 immediately below the reversed polarity Vinegar Hill Tephra (1.75 ± 0.13 Ma) (Naish et al. 1996). Vinegar Hill Tephra has not been identified in the drill core or adjacent Nukumaru coastal section sediments. While the base of the Olduvai normal Subchron is not constrained by the palaeomagnetic data from the drill core, intermediate polarities do trend towards reverse polarities between 80 and 85 m near the base of basin cycle 14, at the base of the Tewkesbury Formation. Basin cycle 14 is correlated with MIS 71 near the base of the Olduvai Subchron in deep sea records (e.g., Shackleton et al. 1990).

Fig. 7 Summary composite log of the Castlecliff-1/1A drill core and borehole shows neutron porosity (NPHI), density (RHO8), and natural gamma (EHGR) digital logs, synthetic seismic well-tie, lithological log, sequence stratigraphic interpretation, isotope stratigraphy, lithostratigraphy, environmental, and palaeobathymetric interpretations. ➤

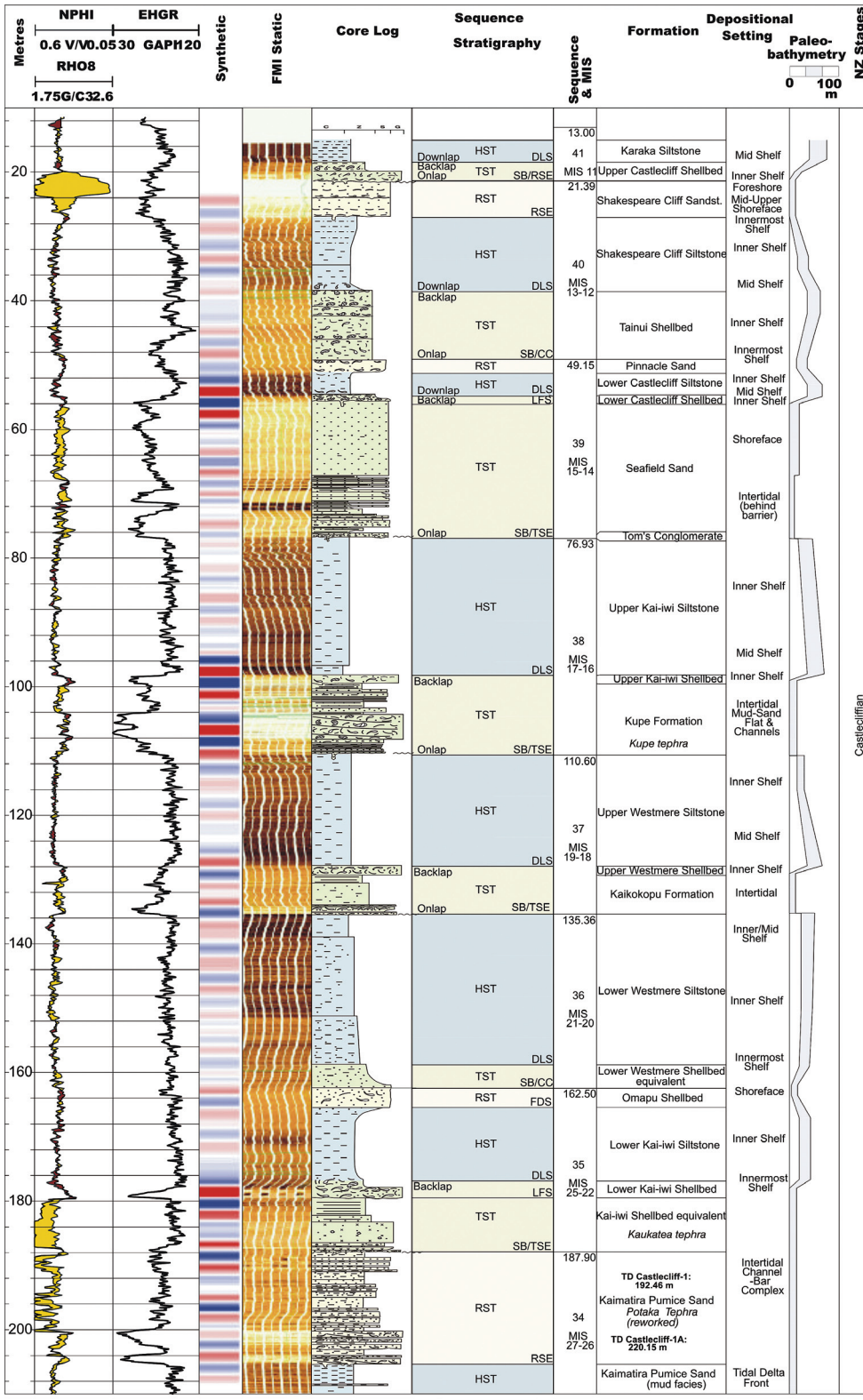
Metres
NPHI
0.6 V/V0.05
RHO8
1.75G/C32.6
EHGR
30 GAPI120
Synthetic
FMI Static
Core Log
Sequence Stratigraphy
Sequence & MIS
Formation
Depositional Setting
Paleo-bathymetry
0 100 m
NZ Stages
20
40
60
80
100
120
140
160
180
200
HST
Downlap
Backlap
Onlap
TST
SB/RSE
RST
RSE
DLS
SB/CC
LFS
SB/TSE
FDS
13.00
41
MIS 11
21.39
40
MIS 13-12
49.15
39
MIS 15-14
76.93
38
MIS 17-16
110.60
37
MIS 19-18
135.36
36
MIS 21-20
162.50
35
MIS 25-22
187.90
34
MIS 27-26
Karaka Siltstone
Upper Castlecliff Shellbed
Shakespeare Cliff Sandst.
Shakespeare Cliff Siltstone
Tainui Shellbed
Pinnacle Sand
Lower Castlecliff Siltstone
Lower Castlecliff Shellbed
Seafield Sand
Tom's Conglomerate
Upper Kai-iwi Siltstone
Upper Kai-iwi Shellbed
Kupe Formation
Kupe tephra
Upper Westmere Siltstone
Upper Westmere Shellbed
Kaikokopu Formation
Lower Westmere Siltstone
Lower Westmere Shellbed equivalent
Omapu Shellbed
Lower Kai-iwi Siltstone
Lower Kai-iwi Shellbed
Kai-iwi Shellbed equivalent
Kaukatea tephra
TD Castlecliff-1: 192.46 m
Kaimatira Pumice Sand
Potaka Tephra (reworked)
TD Castlecliff-1A: 220.15 m
Kaimatira Pumice Sand (mud facies)
Mid Shelf
Inner Shelf
Foreshore
Mid-Upper Shoreface
Innermost Shelf
Shoreface
Intertidal (behind barrier)
Intertidal Mud-Sand Flat & Channels
Intertidal
Inner/Mid Shelf
Intertidal Channel -Bar Complex
Tidal Delta Front
Castlecliffian

Table 1 Sedimentary lithofacies of the Pliocene-Pleistocene Castlecliff and Nukumaru coastal outcrop sections.

Lithofacies association	Code	Description	Depositional environment
Mudstone	Z1	Blue-grey, sparsely to moderately fossiliferous, massive, bioturbated mudstone.	Shelf
	Z2	Blue-grey, massive, bioturbated, moderately fossiliferous sandy mudstone.	Inner shelf
	Z3	Blue-grey, normally graded, centimetre to decimetre scale fine sand and fine sandy-mudstone beds (mud dominated).	Storm-influenced inner shelf
	Z4	Blue-grey, wavy to streaky-laminated/bedded sandy mudstone.	Inner shelf
	Z5	Purple-brown, mottled, barren, massive to weakly-laminated carbonaceous mudstone, with disseminated organic material and plant remains	Non-tidal swamp/ overbank lacustrine
	Z6	Green-grey, barren, organic rich, wavy to lenticular laminated/bedded mudstone.	Supratidal salt marsh
	Z7	Brown to dark-brown lignite.	Swamp
	Z8	Grey-brown, barren to moderately fossiliferous, massive to lenticular/wavy-laminated/bedded, mudstone (often as drapes).	Intertidal channel/flat
Sandstone	S1	Grey, barren to sparsely fossiliferous, bioturbated, massive silty-fine sandstone.	Inner shelf
	S2	Grey, sparsely fossiliferous, barren to weakly bioturbated, wavy-streaky-laminated (symmetrical wave ripples) sandstone and siltstone (sand dominated).	Inner to innermost shelf
	S3	Grey-brown barren to moderately fossiliferous, bioturbated massive fine sandstone.	Innermost shelf, transitional to shoreface
	S4	Grey-brown barren to moderately fossiliferous, bioturbated, crude decimetre scale horizontal to low angle planar cross-stratified fine sandstone.	Innermost shelf, transitional to shoreface
	S5	Grey-brown barren to moderately fossiliferous, moderately bioturbated, well sorted horizontal to low angle planar cross-stratified fine sandstone.	Foreshore/beach
	S6	Grey-brown barren to moderately fossiliferous, moderately bioturbated, medium scale, uni-directional and bi-directional trough-cross stratified fine to medium sandstone.	Shoreface/subtidal channel
	S7	Grey to brown, barren to moderately fossiliferous, moderately bioturbated, flaser bedded/laminated fine to medium sandstone.	Intertidal sand flat
	S8	Grey to brown, high angle planar cross-stratified fine to medium sandstone.	Subtidal lower shoreface bar
	S9	Purple-brown to dark brown palaeosol with incipient pedogenic structure, rootlets and disseminated organic material.	Coastal plain
	S10	Purple-brown, mottled, barren, massive to weakly laminated, carbonaceous sandstone with disseminated organic material and plant remains.	Non-tidal swamp/overbank/ lacustrine
	S11	Grey to brown, barren to sparsely fossiliferous, bioturbated, asymmetrical (current) and symmetrical (wave), well sorted, ripple laminated/bedded fine sandstone.	Shoreface
	S12	White-grey, sparsely fossiliferous to fossiliferous, large scale, trough cross-stratified, pumiceous, pebbly sandstone with mud drapes.	Subtidal channel/Tidal delta front
	S13	Reddish-brown, well sorted, non-fossiliferous, non-bioturbated, high angle planar cross-stratified (dune forms) medium to fine sandstone.	Aeolian sand dune
	S14	Reddish-brown, poorly sorted, non-bioturbated, high angle planar cross-stratified and small to medium trough cross-stratified sandstone and pebbly sandstone.	Fluvial bar and channel
Shellbed	Cz1	Bands, clumps and scattered, often monospecific *in situ* molluscs within bioturbated massive siltstone to fine sandy siltstone.	Inner to mid shelf
	Cz2	Closely packed molluscan shells within bioturbated terrigenous fine sandy siltstone.	Inner to mid shelf
	Cs1	Closely packed molluscan shells within bioturbated terrigenous fine sandstone or silty-fine sandstone.	Inner shelf to shoreface
	Cs2	Closely packed, cross-stratified shell pebble conglomerate or pebbly sandstone. Includes old and new abraded molluscs, intraclasts, greywacke pebbles within a coarse sand matrix. May also include mud drapes.	Shoreface/subtidal channel/delta
	Cs3	Bands, clumps and scattered, often monospecific *in situ* molluscs within bioturbated massive silty-fine sandstone and siltstone.	Inner shelf

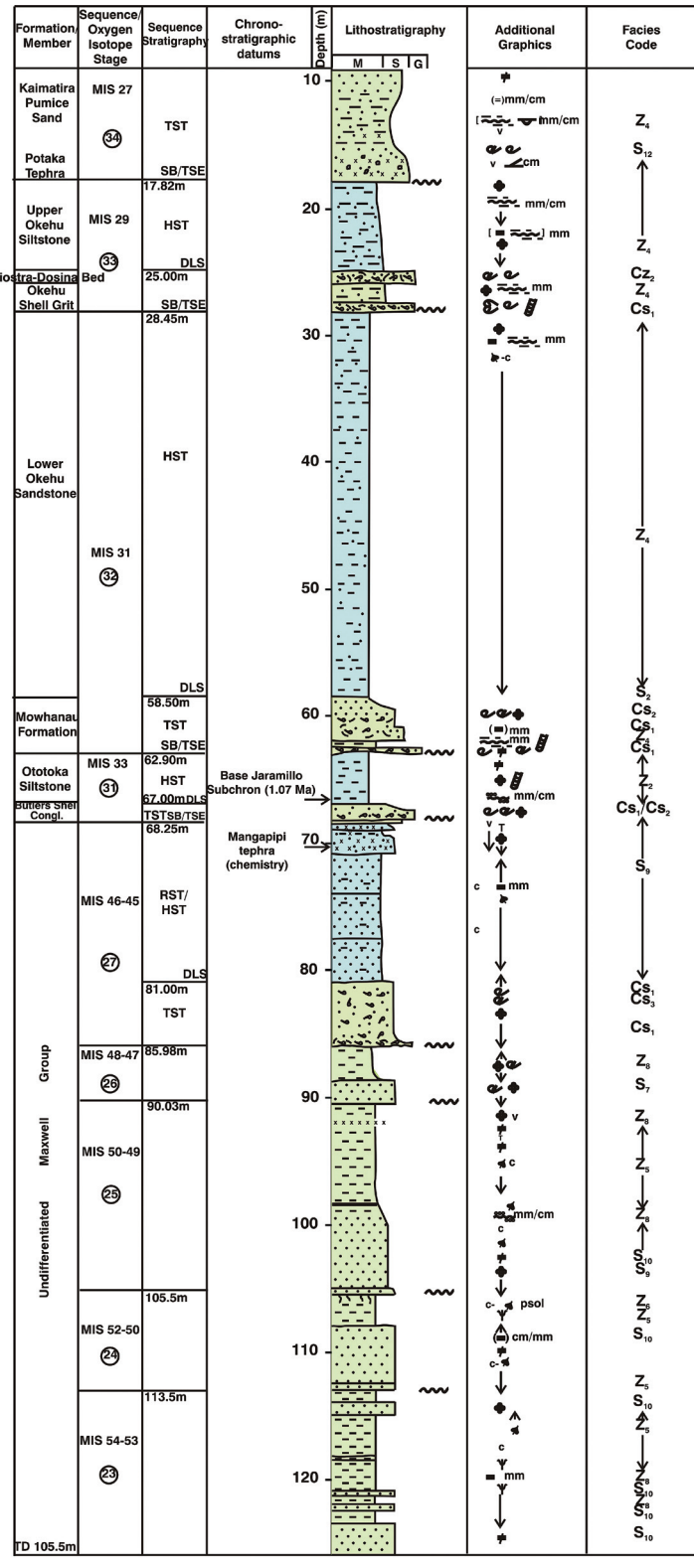

Fig. 8 Summary composite log of the Kai-iwi-1 drill core shows lithological log, sequence stratigraphic interpretation, isotope stratigraphy, lithostratigraphy, and facies interpretations.

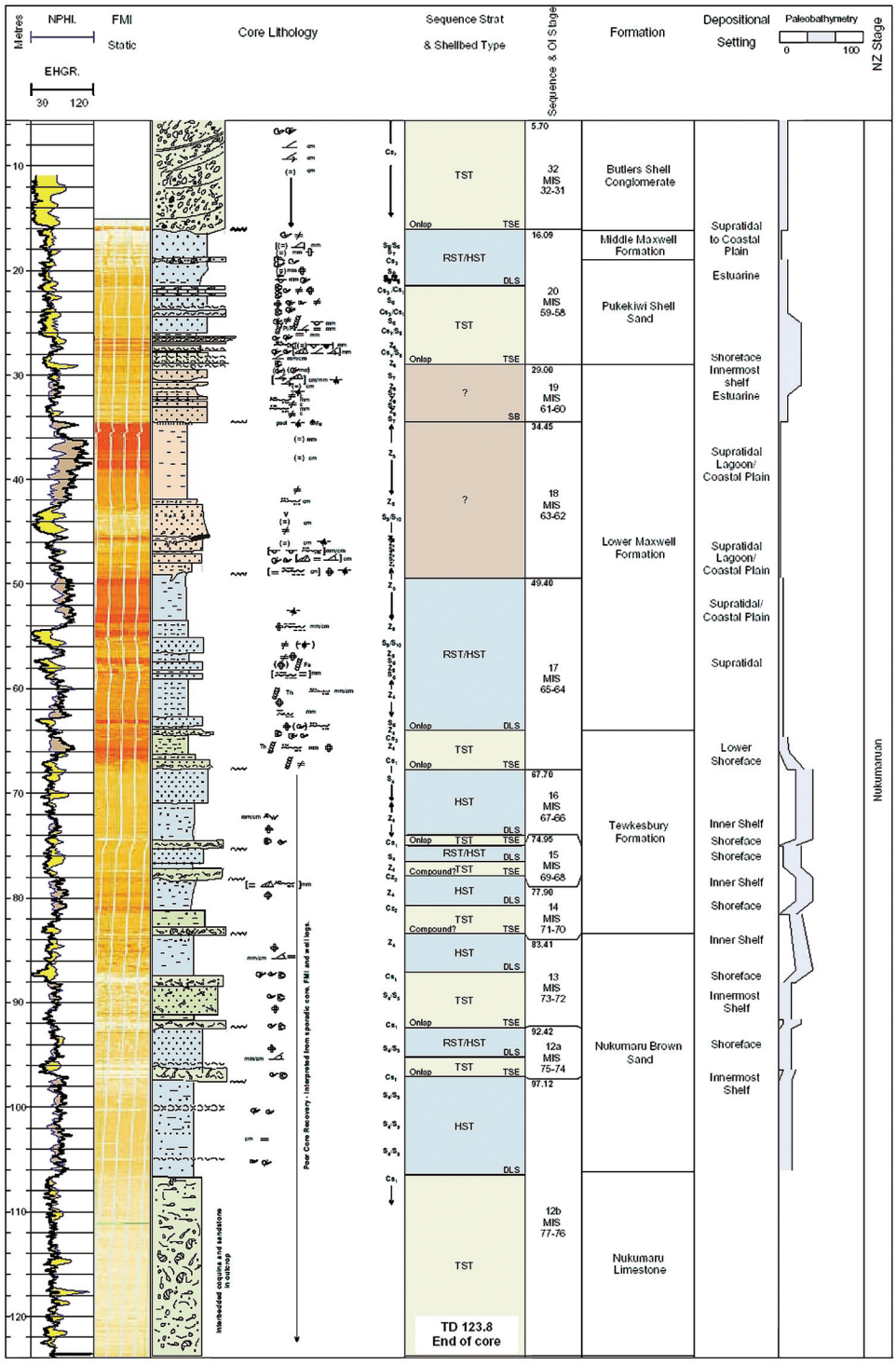

Fig. 9 Summary composite log of the Ototoka-1 drill core and borehole shows neutron porosity (NPHI), and natural gamma (EHGR) digital logs, synthetic seismic well-tie, lithological log, sequence stratigraphic interpretation, isotope stratigraphy, lithostratigraphy, environmental, and palaeobathymetric interpretations.

Tephrochronology

The distal record of late Neogene, silicic arc volcanism in central North Island, recorded in Wanganui and other New Zealand sedimentary basins, is now well established (e.g., Alloway et al. 1993; Pillans et al. 1994; Naish et al. 1996; Shane et al. 1996; Alloway et al. 2005; Pillans et al. 2005 this issue). Many of the volcaniclastic horizons (tephra) are similar in field appearance, but chemical fingerprinting of the glass shards (Pillans et al. 1994, 2005 this issue), allows most to be distinguished. Many of the tephra have correlatives in deep sea cores off eastern New Zealand (e.g., Nelson et al. 1986; Carter et al. 1995; Carter et al. 2003; Alloway et al. 2005), where high resolution orbitally tuned chronologies contribute to the quality of the tephrochronology for onland Wanganui Basin deposits.

Glass shards from 10 silicic volaniclastic horizons in the Castlecliff and Kai-iwi cores were analysed by electron microprobe for nine major elements (Table 2). Major oxide chemistry of the glass shards reveals ranges for SiO_2 of 74–78 wt% and $K_2O + Na_2O$ of 6–9 wt%, when the shard compositions are averaged (n = 15–20) and recalculated to 100% on a water free basis. Using the compositional classification scheme of Le Maitre (1984), all Wanganui drill core tephra occur within the rhyolite field and are identical to other onshore and offshore Taupo Volcanic Zone deposits. All the tephra were compositionally homogeneous, with respect to inter-shard variation, implying that they were erupted from a single event. The stratigraphic position and distinctive major element oxide composition, such as FeO and CaO (wt%), allow the tephra horizons between 187.03–182.23 m in Castlecliff-1A and 68.65–68.22 m Kai-iwi-1 to be correlated with the Kaukatea Tephra (0.87 ± 0.05 Ma) and Mangapipi Tephra (1.51 ± 0.16 Ma), respectively (Table 2).

Identification of primary Kaukatea Tephra at the level of the Lower Kai-iwi Shellbed in basin cycle 35 (MIS 23) of Castlecliff-1A (Fig. 7) is consistent with the stratigraphic position and age of primary Kaukatea Tephra in the Turakina Valley section (Alloway et al. 2005; Pillans et al. 2005 this issue), and its occurrence as reworked pumiceous glass in Lower Kai-iwi Shellbed in the Castlecliff coastal section. The identification of Mangapipi Tephra in the cycle immediately underlying the Butlers Shell Conglomerate (correlative) in Kai-iwi-1 (Fig. 8) implies correlation of the cycle with MIS 53, based on correlation of the Mangapipi tephra elsewhere in Wanganui Basin with the oxygen isotope record (Alloway et al. 2005; Pillans et al. 2005 this issue). A consequence of this is that Kai-iwi-1 comprises a stratigraphic record of basin cycles 23–27, which are also recorded in the Turakina and Rangitikei sections, but are missing in coastal outcrop below the Butlers Shell Conglomerate. This further emphasises the restricted nature of the coastal unconformity (described below).

Integrated chronostratigraphy and cyclostratigraphy for the composite cored succession

Tephra correlations described above, and their numeric ages, are consistent with the palaeomagnetic interpretation and cyclostratigraphy of the drill core record, and provide important constraints for stratigraphic correlation of the three cored successions into a composite record. A minor overlap was achieved between the base of Castlecliff-1A and the top of the Kai-iwi-1 cores, as evidenced by the occurrence at both sites of Kaimatira Pumice Sand/Potaka Tephra within normal polarity (Jaramillo Subchron) basin cycle 34. In contrast, significant overlap was achieved between the Kai-iwi-1 and Ototoka-1 drill cores. The base of the Butlers Shell Conglomerate (basin cycle 31), which occurs at 68.25 m in Kai-iwi-1, occurs at 16.09 m in Ototoka-1. Intriguingly, the 450 ka duration unconformity at the base of the Butlers in Ototoka-1, and exposed in outcrop at Ototoka Beach (equivalent to basin cycles 23–30 (MIS 57–30)), only spans c. 120 ka in Kai-iwi-1. Here, only basin cycles 28–30 (MIS 44–32) are not represented. The 40 m thick stratigraphic record below the Butlers Shell Conglomerate in Kai-iwi-1 represents a new non-marine to marginal marine record of basin cycles 23–27,

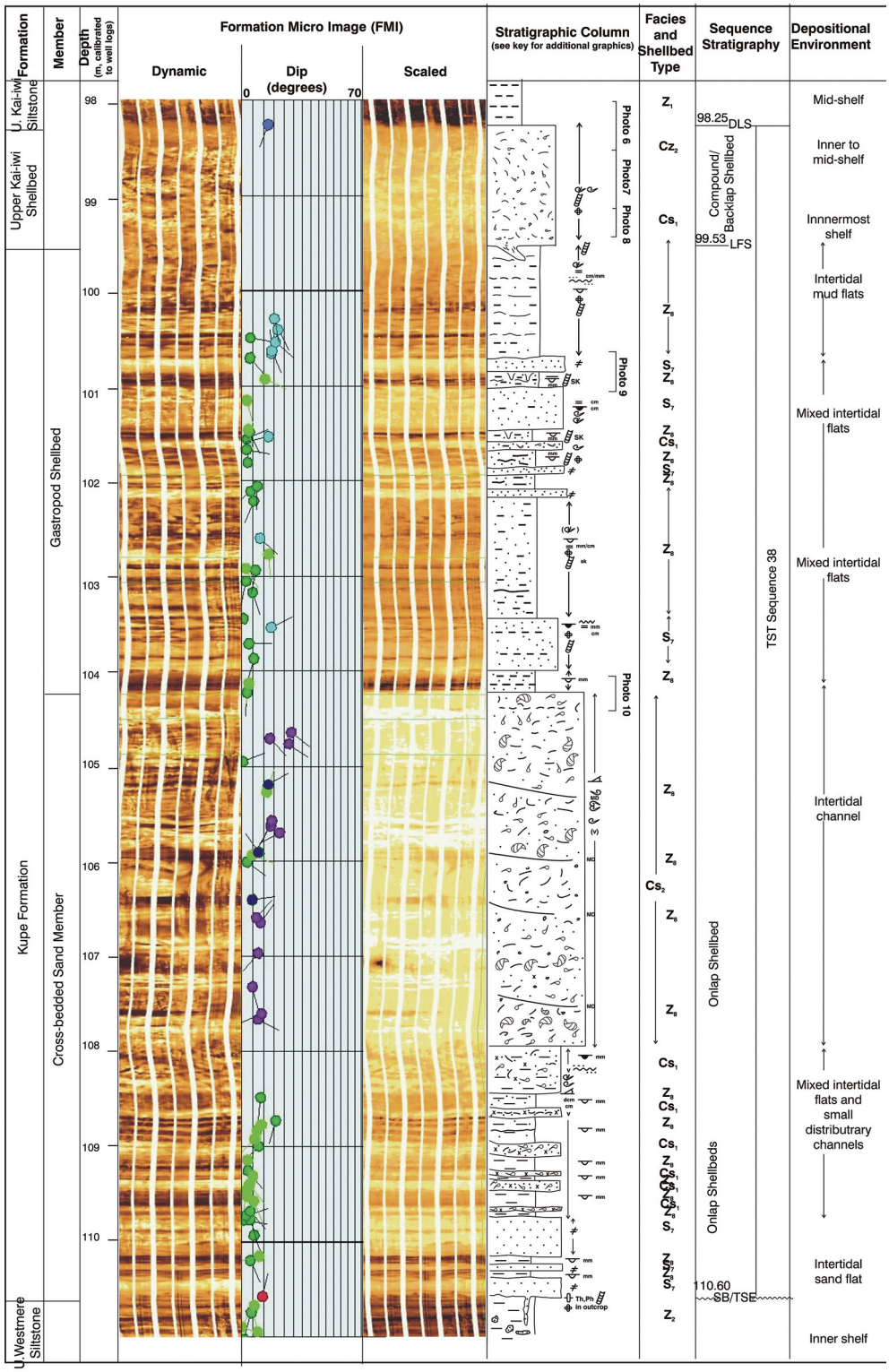
Formation
Member
Depth (m, calibrated to well logs)
Formation Micro Image (FMI)
Dynamic
Dip (degrees)
0
70
Scaled
Stratigraphic Column (see key for additional graphics)
Facies and Shellbed Type
Sequence Stratigraphy
Depositional Environment
U. Kai-iwi Siltstone
Upper Kai-iwi Shellbed
Gastropod Shellbed
Cross-bedded Sand Member
Kupe Formation
U. Westmere Siltstone
98
99
100
101
102
103
104
105
106
107
108
109
110
Photo 6
Photo7
Photo 8
Photo 9
Photo 10
98.25 DLS
99.53 LFS
110.60 SB/TSE
Compound/ Backlap Shellbed
TST Sequence 38
Onlap Shellbed
Onlap Shellbeds
Mid-shelf
Inner to mid-shelf
Innnermost shelf
Intertidal mud flats
Mixed intertidal flats
Mixed intertidal flats
Intertidal channel
Mixed intertidal flats and small distributrary channels
Intertidal sand flat
Inner shelf

equivalent to MIS 53–44. The seismic stratigraphy, described below, indicates complex stratal geometries, with localised erosion of basin cycles 21–31.

The stratigraphic splicing of the three cored successions, together with the sequence stratigraphic and lithostratigraphic interpretations outlined above, allows a robust correlation of the behind-outcrop drill core record with the outcropping coastal stratigraphy. The vertical occurrence of facies and shellbeds, and the sequence architecture described above for the Castlecliff-1A drill core is remarkably similar to the stratigraphy of the outcropping sediments. Lithostratigraphic units, sequences, and systems tracts in the cored succession can be readily correlated with those recognised in the outcrop down to the level of the Lower Kai-iwi Shellbed (c. 180 m). Below this the increasing down dip distance between the outcrop and the drill core leads to lateral facies variations and a more complete record of the volcaniclastic rich basin cycles 34 (containing Kaimatira Pumice Sand) and 35 (containing Kaukatea Tephra).

Likewise, lithostratigraphic units, sequences, and systems tracts in Kai-iwi-1 can be readily correlated with the coastal outcrop stratigraphy between the Kaimatira Pumice (basin cycle 34) and the base of the Butlers Shell Conglomerate (basin cycle 31) due to the stratigraphic proximity of the borehole. As described above, a new record of basin cycles 27–23 was encountered in the lower part of Kai-iwi-1 drill core that are missing at the base of Butlers Shell Conglomerate unconformity in the coastal outcrop.

With the exception of basin cycle 21, which contains the Ototoka Tephra in the coastal section, a one-to-one match can be made between the outcrop stratigraphy (Abbott et al. 2005 this issue) and the lithostratigraphy and sequence stratigraphy of the Ototoka-1 drill core. Local relief at a scale of several metres on the channelled unconformity beneath the Butlers Shell Conglomerate removes basin cycle 21 in the vicinity of the Ototoka-1 drill site (Fig. 4C). In contrast, 200 m south-east of the Ototoka Stream mouth, the Ototoka Tephra is well exposed in coastal cliffs within non-marine Upper Maxwell Formation (Fig. 4B). While poor core recovery hampered interpretation of the lower part of the Ototoka-1 core, the use of the borehole formation micro-image logs (see below) along with intermittent core allowed recognition of the sequence architecture.

BOREHOLE STRATIGRAPHY

Electric well-log and core-log signatures of depositional sequences

The boreholes were reamed out following completion of coring to allow a suite of digital logs to be recorded by Schlumberger Data Services. Ototoka-1 was logged immediately after drilling in September 1999, and Castlecliff-1A was logged a year later in late 2000. Kai-iwi-1 was not logged due to the unstable nature of the borehole. The purpose of running digital logs was to develop sequence stratigraphic models based on the physical properties of the sediments as expressed by the various geophysical log signatures. Such models have wide application in the analysis of high frequency sequences in petroleum wells where continuous core is not available, and seismic data are typically of too low a frequency to resolve the stratigraphic complexity of many shallow-marine reservoirs.

◀ **Fig. 10** Expanded section from Castlecliff-1/1A borehole and core, showing formation micro-resistivity logs and dip measurements for the cored interval between 111 and 98 m. Dip measurement colours are red for sequence boundaries, blue for downlap surfaces, orange for regressive surfaces of erosion, purple for mud drapes, light blue for cross-stratification, green for horizontal and low angle planar stratification. Detailed facies logs and environmental interpretations are based on Table 1. Core photos are shown in Fig. 12.

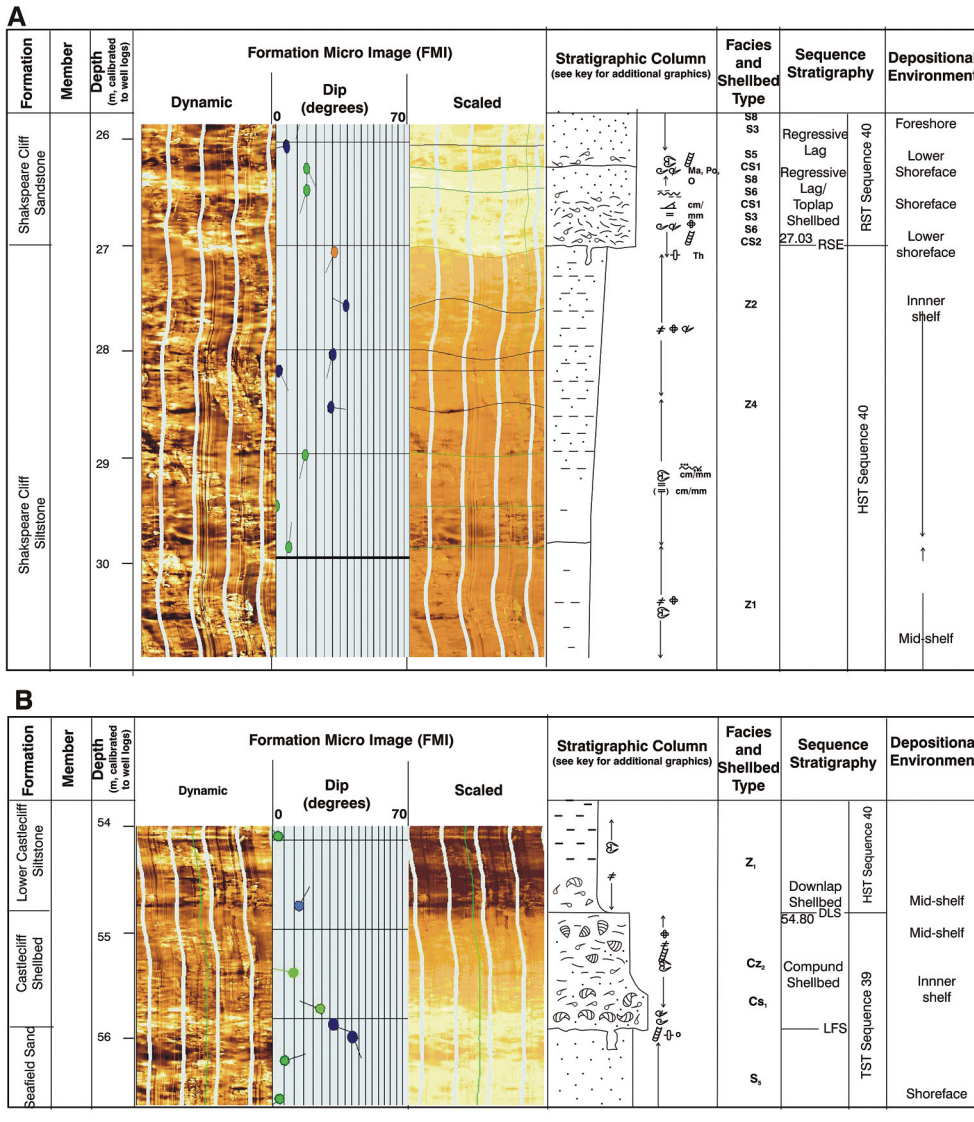

Fig. 11 Expanded sections from Castlecliff-1/1A borehole and core, showing formation micro-resistivity logs and dip measurements for the cored intervals between (**A**) 56.5–54 m and (**B**) 31–26 m. Dip measurement colours are red for sequence boundaries, blue for downlap surfaces, orange for regressive surfaces of erosion, purple for mud drapes, light blue for cross-stratification, green for horizontal and low angle planar stratification. Detailed facies logs and environmental interpretations are based on Table 1.

The complete suite of wireline logs is shown on large format posters for the boreholes and can be accessed from the following website www.gns.cri.nz/. Only neutron porosity, density, and gamma logs are shown on well composite summaries in Fig. 7 and 9. The two caliper logs, CALI 1 and CALI 2 (or C1 and C2), record variations in the diameter of the hole across two orthogonal axes. Well sorted, friable sandstone intervals, with high water contents, were typically associated with borehole collapse and caving.

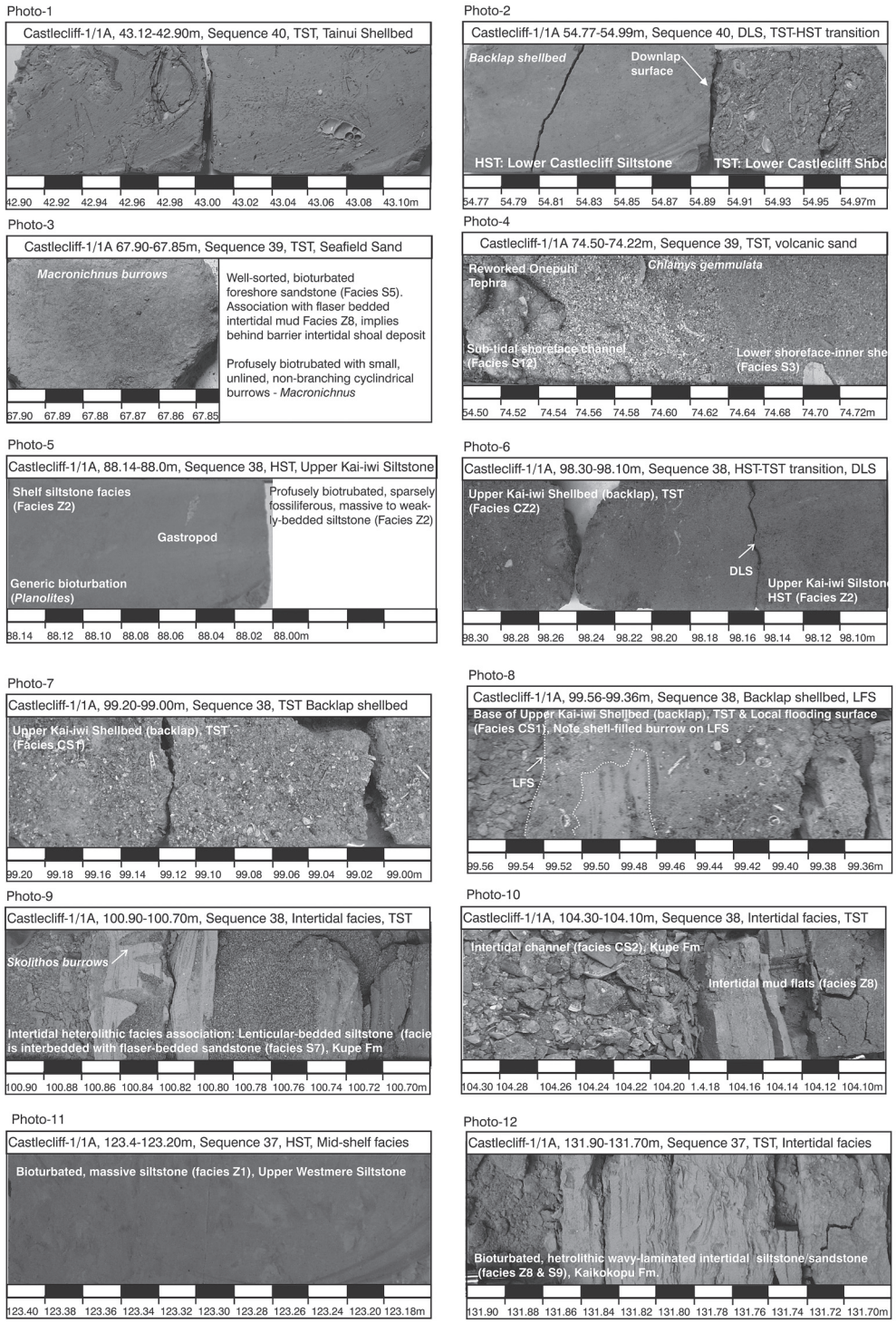

Fig. 12 Photographs of Castlecliff-1/1A core highlight sequence stratigraphic and facies features discussed in text and shown in Fig. 10. Scale bars in 1 and 2 cm divisions are indicated for each core interval.

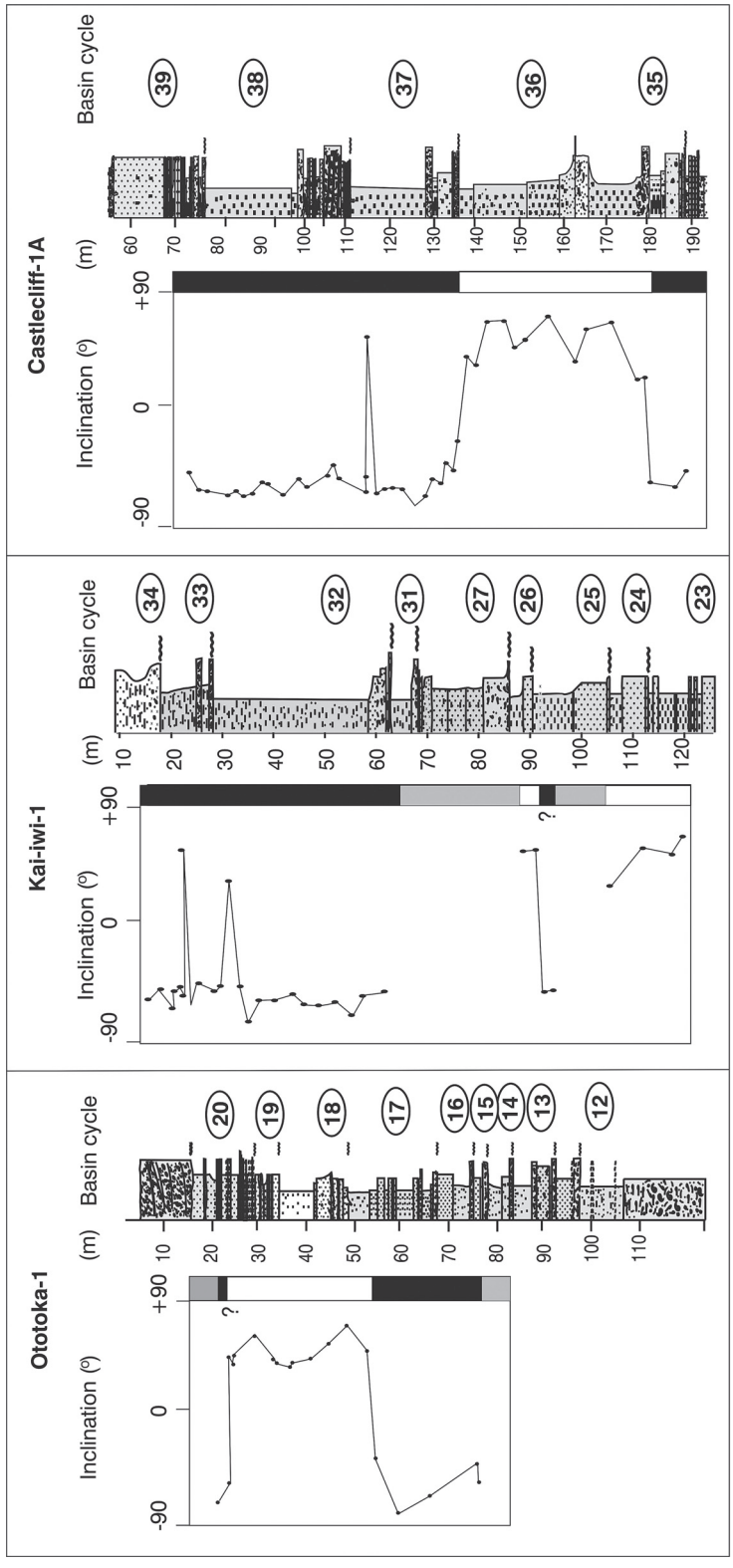

Fig. 13 The magnetic polarity zonation of the three drill cores. Black represents normal polarity and white represents reversed polarity. Grey represents intervals for which it was not possible to determine the remanent magnetisation.

The neutron log (NPHI) records the density of hydrogen atoms and gives high readings where the formation contains more water (or hydrocarbons), and displays higher porosity. The density log (RHO8) records variations in the bulk density of the rock, and the difference between the NPHI and RHO8 logs is a standard way of highlighting zones of higher porosity. Another effective way of highlighting sequence architecture on the basis of sand/porosity content is to overlay the natural gamma log on the density log (e.g., Fig. 9).

Environmentally corrected, high resolution natural gamma ray (EHGR) log displays variations in the natural radioactivity of the sediments. Fine grained, clay rich shelf mudstones typically contain higher uranium and potassium than quartz rich and plagioclase rich shallow water sandstones and carbonates. Figure 7 shows the strong relationship between the stratigraphic architecture of the shallow-marine sequences and the gamma-ray log for Castlecliff-1A. Sequence boundaries marking abrupt transitions from HST shelf siltstone to shallow water TST shellbeds and sandstones, correspond to abrupt negative shifts on the EHGR log. Transgressive sandstones and shellbeds exhibit low gamma-ray values that increase abruptly across the downlap surface to maximum values in the finest grained sediments near the base of the HST, corresponding to maximum palaeowater depths. Most HSTs show a small progressive decrease in gamma-ray values as sand content increases up section. However, in some cases the upper parts of sequences have not been truncated, and HST-RST transition is abruptly gradational, and coarsens from innermost shelf muddy sandstone to well sorted sandy shoreface and foreshore facies (e.g., basin cycle 40, Shakespeare Cliff Siltstone-Shakespeare Cliff Sandstone). Here, the gamma ray values decrease dramatically towards the top of the sequence. Natural gamma provides an extremely sensitive proxy for the sequence boundary, downlap surface and transgressive-regressive facies successions within shallow-marine depositional sequences.

A number of other wireline logs were run, but are only shown on the website and include: (1) water saturation log (SW_HILT) derived from resistivity and porosity logs; (2) shallow laterolog resistivity log (HLLS), also useful for identifying water rich, porous zones or the presence of clays, and (3) the sonic log (DT), which records the transit time of a compressional wave in the rock, along the borehole wall.

Magnetic susceptibility logs were run on the split core using a GEOTEK multi sensor core logger at the Institute of Geological and Nuclear Sciences. Magnetic susceptibility measurements and data processing followed the procedures of Niessen et al. (1998). In general, high values of magnetic susceptibility were associated with volcaniclastic horizons.

Formation micro-resistivity image analysis of depositional sequences

The formation micro-resistivity image (FMI from Schlumberger's FBST-B tool) log records variations in resistivity in the borehole wall with the resolution of a few millimetres. Some 192 detectors each take one reading every 2.5 mm as the sonde is raised slowly up the hole. Software uses inclination and azimuthal data (from a magnetometer) and other coeval readings to compile the resistivity values into a pseudo-image of the borehole wall, where the colour palette reflects high resolution variations in resistivity. Such changes are related to changes in lithology and can reveal bedding surfaces, sedimentary structures within beds, burrows and fractures. More resistive readings are conventionally shown in yellow and commonly denote sand rich horizons (or concretions); mudstones are commonly more conductive and appear brown. Dipping surfaces detected with the FMI tool appear as sinusoids on the image log and the amplitude and position of the sinusoids can be used to compute the dip and strike of the feature.

Table 2 Major element glass composition of silicic tephra beds retrieved from Castlecliff and Kai-iwi cores compared with their tephra

	SiO_2	Al_2O_3	TiO_2	FeO	MgO	MnO	CaO	Na_2O	K_2O	Cl	H_2O	*n*
CASTLECLIFF CORE												
Kaukatea Correlatives												
AT-417	77.56	13.02	0.14	1.58	0.12	0.06	0.95	4.31	3.34	0.19	7.13	16
Redeposited unit, 182.23 m	0.22	0.13	0.05	0.04	0.03	0.03	0.04	0.17	0.10	0.02	0.72	
AT-418	77.37	13.09	0.16	1.59	0.12	0.06	0.97	4.30	3.41	0.19	7.20	15
Redeposited unit, 183.62 m	0.21	0.13	0.04	0.06	0.04	0.03	0.04	0.21	0.19	0.02	0.63	
AT-419	77.40	13.04	0.14	1.55	0.13	0.05	0.96	4.20	3.59	0.21	7.81	15
Redeposited unit, 184.15 m	0.63	0.23	0.04	0.20	0.04	0.02	0.11	0.37	0.21	0.05	1.57	
AT-420	76.71	13.00	0.15	1.51	0.12	0.05	0.97	4.33	3.55	0.19	7.48	16
Redeposited unit, 185.30 m	0.43	0.20	0.04	0.13	0.05	0.03	0.05	0.18	0.22	0.02	1.24	
AT-421	76.64	13.12	0.14	1.56	0.12	0.07	0.96	4.32	3.46	0.19	7.38	13
Redeposited unit, 185.65 m	0.45	0.22	0.03	0.12	0.03	0.03	0.08	0.20	0.19	0.02	0.61	
AT-422	76.57	13.10	0.14	1.58	0.13	0.07	0.99	4.39	3.41	0.19	7.10	16
Airfall unit (upper), 186.87 m	0.37	0.17	0.07	0.06	0.05	0.02	0.06	0.14	0.16	0.02	1.00	
AT-423	76.68	13.04	0.14	1.58	0.13	0.06	0.97	4.46	3.32	0.19	6.83	16
Airfall unit (lower), 187.03 m	0.19	0.10	0.04	0.05	0.03	0.02	0.04	0.14	0.12	0.02	0.91	
BP-478/16*	76.27	12.77	0.22	1.63	0.16	–	1.07	4.27	3.40	0.21	6.25	11
Turakina Valley (S22/069342)	0.39	0.16	0.03	0.15	0.03		0.16	0.16	0.25	0.03	1.21	
BP-468*	76.60	12.72	0.13	1.54	0.12	–	0.98	4.28	3.44	0.19	5.35	22
Longacre Rd (S22/901424)	0.33	0.08	0.04	0.12	0.02		0.05	0.19	0.25	0.04	0.77	
AT-289	76.72	13.03	0.13	1.62	0.12	0.09	1.02	3.83	3.28	0.16	5.53	16
ODP-1125, 20.96 mcd	0.29	0.08	0.08	0.08	0.02	0.04	0.03	0.21	0.11	0.03	0.74	
AT-280	76.61	13.07	0.16	1.58	0.12	0.06	0.99	3.87	3.37	0.15	4.34	15
ODP-1122, 322.94 mcd	0.30	0.12	0.07	0.06	0.02	0.05	0.08	0.45	0.23	0.03	0.67	
Kidnappers-B Correlatives												
AT-424	77.12	12.70	0.13	1.46	0.12	0.08	0.96	4.08	3.71	0.24	7.70	5
Redeposited unit, 192.26 m	0.95	0.52	0.07	0.38	0.01	0.01	0.12	0.38	0.45	0.06	1.31	
BP-478/11A*	76.26	12.85	0.17	1.66	0.15	–	1.15	4.01	3.57	0.18	6.55	8
Whangaehu Valley (S22/028382)	0.25	0.17	0.03	0.08	0.06		0.06	0.15	0.11	0.05	0.64	
9†	76.10	12.89	0.18	1.55	0.14	–	1.06	4.35	3.57	0.16	5.91	24

Cape Kidnappers	0.22	0.09	0.04	0.08	0.03		0.06	0.13	0.13	0.03	0.86	
AT-490	76.51	13.03	0.18	1.54	0.14	–	1.08	3.94	3.41	0.11	5.43	29
ODP-1124, 37.56 mcd	0.76	0.31	0.08	0.28	0.04		0.16	0.18	0.19	0.04	1.15	
AT-491	76.09	13.11	0.18	1.69	0.14	–	1.04	4.23	3.33	0.11	4.97	27
ODP-1124, 39.68 mcd	0.60	0.24	0.08	0.21	0.04		0.13	0.13	0.11	0.04	1.36	
AT-285	76.66	12.97	0.18	1.61	0.15	–	1.19	3.63	3.42	0.13	5.43	16
ODP-1125, 21.79 mcd	0.47	0.21	0.07	0.13	0.04		0.11	0.14	0.19	0.03	0.65	
KAI-IWI CORE												
Mangapipi Correlatives												
AT-425	74.95	13.59	0.17	2.30	0.12	0.08	1.14	4.71	3.29	0.22	7.67	16
Airfall unit, 68.22 m	0.23	0.14	0.04	0.07	0.03	0.04	0.04	0.20	0.09	0.03	1.16	
AT-426	74.63	13.65	0.18	2.21	0.12	0.09	1.12	4.51	3.34	0.20	6.70	15
Redeposited unit, 68.65 m	0.27	0.14	0.06	0.09	0.02	0.03	0.05	0.31	0.36	0.02	0.77	
UT-1157	74.24	13.53	0.22	2.24	0.16	–	1.20	4.64	3.49	0.24	6.26	13
Rangitikei (T22355345)	0.32	0.16	0.05	0.15	0.03		0.08	0.12	0.12	0.05	0.88	
AT-355	74.74	13.62	0.21	2.26	0.14	–	1.23	4.06	3.58	0.15	5.38	14
Rangitikei (T22/352344)	0.27	0.10	0.06	0.09	0.02		0.07	0.21	0.11	0.02	0.81	
AT-356	74.89	13.61	0.19	2.25	0.15	–	1.17	4.11	3.47	0.16	5.31	15
Rangitikei (T22/352343)	0.27	0.06	0.08	0.10	0.02		0.09	0.14	0.15	0.02	0.73	
Uncorrelated												
AT-427	77.22	12.57	0.10	1.41	0.05	0.06	0.71	3.66	4.04	0.23	6.00	5
Redeposited unit 68.95 m	0.68	0.14	0.03	0.05	0.01	0.04	0.02	0.78	0.08	0.02	0.92	
Glass Standard (UA-5831)	74.82	13.25	0.08	1.59	0.04	0.07	0.73	4.06	5.09	0.36	1.10	39
May01.3-std	0.30	0.09	0.04	0.06	0.01	0.03	0.03	0.29	0.09	0.03	0.51	
Glass Standard (UA-5831)	73.83	13.08	0.07	1.57	0.05	0.07	0.72	4.08	4.99	0.35	1.27	29
May01.2-std	1.27	0.29	0.03	0.04	0.03	0.03	0.03	0.12	0.07	0.02	1.60	

Analyses made using a Cameca SX-50 wavelength dispersive microprobe operating at 15 keV accelerating voltage and housed at the University of Toronto. Beam current of 15 nA and a 10-20 μm beam diameter were used for all analyses. All elements calculated on a water free basis, with H_2O by difference from 100%. All Fe expressed as FeO. Mean and ± 1 SD based on *n* analyses. Analyst: B. V. Alloway, *B.J. Pillans, † P. A. Shane.
correlatives.

The full FMI logs for Castlecliff-1A and Ototoka-1 are shown in Fig. 7 and 9, respectively, as a static image which utilises a fixed range of colour intensities corresponding to resistivity values for the borehole. This type of static FMI image, at the sequence-scale, highlights dramatically the abrupt lithological transitions associated with sequence boundaries and downlap surfaces, and broad-scale facies successions within sequences. For example, the coarsening-upwards, shelf mudstone to shoreline sandstone facies assemblage in basin cycle 40 in the upper part of the Castlecliff-1A (Fig. 7) shows a progressive change from a less resistive stratified brown unit to a more resistive stratified yellow to white unit. The FMI log, in combination with the natural gamma log, provide powerful proxies for reconstructing sequence stratigraphic architecture from the borehole.

Expanded high resolution views of the FMI logs for Castlecliff-1A intervals are provided for:

(1) 120–98 m, Upper Westmere Siltstone, Kupe Formation, Upper Kai-iwi Shellbed, Upper Kai-iwi Siltstone; basin cycle 37/38 sequence boundary, cycle 38 TST and TST-HST transition (Fig. 10).
(2) 31–26 m, Shakespeare Cliff Siltstone, Shakespeare Cliff Sandstone; basin cycle 40 HST-RST transition (Fig. 11A).
(3) 56.5–54 m, Upper Seafield Sand, Lower Castlecliff Shellbed, Lower Castlecliff Siltstone; basin cycle 39 TST-HST transition (Fig. 11B).

The high resolution study allows centimetre scale and decimetre scale features (bedding, bioturbation, surfaces, fossils) observed in the core to be compared directly with the FMI logs. Photographs of representative bedding, bioturbation features, and sequence stratigraphic surfaces are shown in Fig. 12. The stratigraphic location of some of the core photographs are also annotated on Fig. 8 and 9. Both static and dynamic FMI logs are shown for these expanded intervals of the Castlecliff-1A core. The advantage of the dynamic log is that it utilises a sliding window to adjust image intensity and contrast, which allows the detailed sedimentary features within an individual lithologic unit or facies to be recognised.

The match between the core graphic log and core photos of the borehole stratigraphy is precise, and allows recognition of individual beds of centimetre scale. Heterolithic intertidal lithologies comprising wavy, flaser, and/or lenticular bedding are well defined as alternating bright and dark beds in the FMI log in both the lower and upper parts of Kupe Formation (Fig. 10). The stratigraphically intermediate, tidally deposited, cross-bedded shelly sandstone facies with interbedded mud drapes displays bright mottled units corresponding to shellbeds, and darker sinusoidal beds corresponding to dipping intervening mud drapes. Condensed backlap (or mid-cycle) shellbeds marking the top of TSTs (e.g., Upper Kai-iwi Shellbed) are typically light brown to bright yellow with white mottles corresponding to shells. The Lower Castlecliff Shellbed displays an upward transition from sand supported shellbed to a mud matrix supported shell facies, which is observed as a progressive decrease in resistivity (yellow to brown colour) in the FMI log.

SEISMIC STRATIGRAPHY

Data acquisition

Approximately 12 km of multichannel seismic (MCS) reflection data (GNS Wanganui Line, Fig. 1) were acquired along the beach below the outcrop sections adjacent to coastal cliffs between Castlecliff Beach and a point 3.5 km south-east of the Ototoka Stream mouth. The data were acquired in a series of surveys between 1994 and 1997 conducted by the Institute of Geological and Nuclear Sciences. Twelve-fold coverage was obtained by combining a 48-channel recorder with shot and receiver spacing of 10 and 5 m, respectively. Receivers used

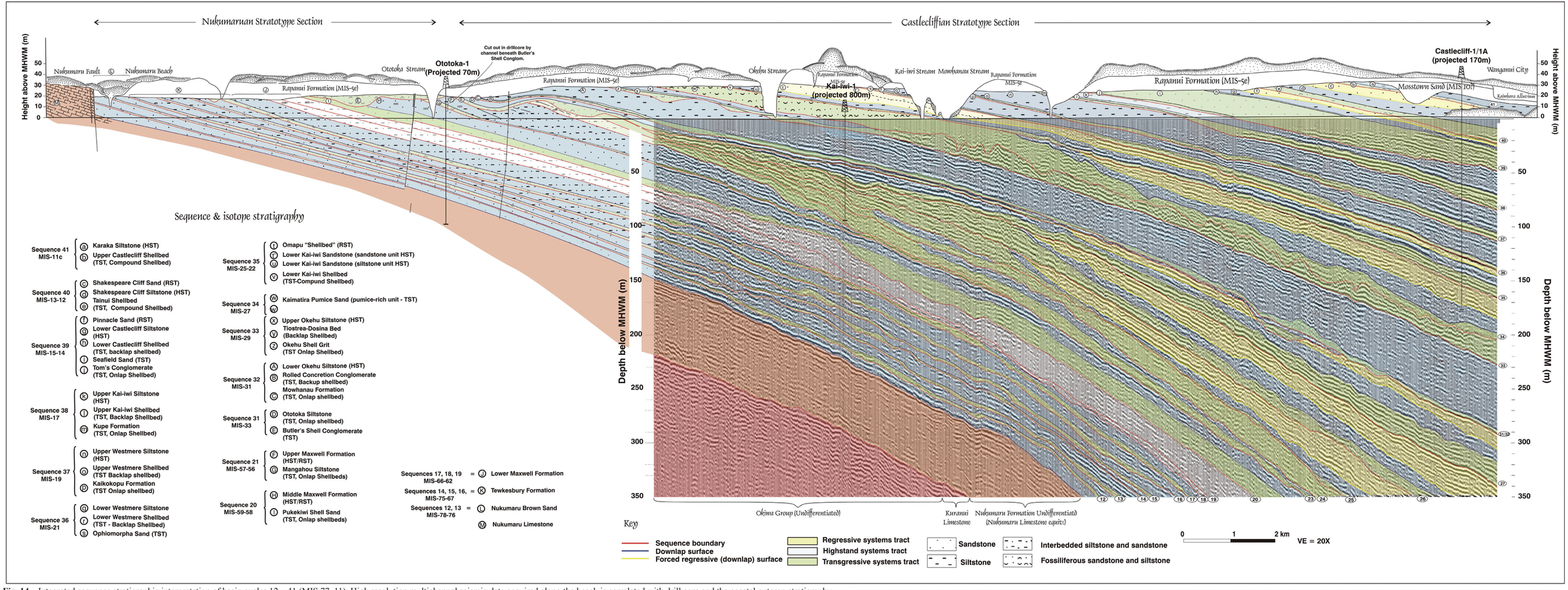

Fig. 14 Integrated sequence stratigraphic interpretation of basin cycles 12 – 41 (MIS 77–11). High resolution multichannel seismic data acquired along the beach is correlated with drill core and the coastal outcrop stratigraphy.

single 100 Hz geophones. A split-symmetric spread geometry was utilised and produced near and far offsets of 2.5 and 117.5 m, respectively. Shots consisted of 80 g of ICI Powergel drilled to 1.5 m below the beach surface and tamped.

Data characteristics

The data quality was excellent due to the absence of a low or variable velocity near-surface layer. The wet sand into which the shots and geophones were placed is a uniform material, with a velocity of 1600 m/s, which provides highly effective source/ground coupling. Processing was performed using Globe Claritas™ processing software (Ravens 1999). The processing stream for individual segments of the GNS Wanganui Line is outlined in detail in Melhuish (1994). The data were subsequently spliced into a single seismic line, reprocessed to optimise resolution, and depth converted using velocity depth models from Castlecliff-1A and Ototoka-1.

The dominant frequency of the reflected energy is around 180 Hz. The velocity in the top c. 100 ms of the section is around 1700 m/s, resulting in a wavelength of 10 m. The vertical resolution is usually taken as a quarter wavelength, so that for these data, boundaries of a unit 2.5 m thick should be visible as separate reflections. The resolution does, however, progressively decrease at greater time intervals, as the velocity increases and the dominant frequency decreases.

Seismic sequence stratigraphy

The depth-converted composite seismic reflection profile is correlated with a 2D section modified from Fleming (1953) for the stratigraphy of the coastal cliffs (Fig. 14). Both seismic and outcrop sections are plotted at the same vertical and horizontal scale, allowing the dipping depositional sequences in the outcrop to be traced into the subsurface seismic profile.

The seismic profile images a well stratified, regionally extensive southeastward-dipping and thickening sedimentary succession. Up to 25 unconformity-bounded depositional sequences are identified in the seismic data between the inferred top of the Nukumaru Limestone (MIS 77, c. 2.05 Ma) and the Karaka Siltstone (MIS 11, c. 0.4 Ma). Individual sequences range from c. 5–50 m thick and comprise three recurring seismic units readily recognised in the majority of the sequences. Internally each sequence comprises, in ascending stratigraphic order:

1. An irregular hummocky to broadly undulating unit up to 20 m thick, containing high amplitude subhorizontal to convex and concave internal reflectors. This unit overlies an erosional unconformity that truncates underlying reflectors and sometimes displays erosional, channelled relief of up to 10 m. The upper bounding surface is subhorizontal, shows no sign of erosion, but sometimes displays a hummocky relief. This unit is interpreted as coarse grained transgressive coastal deposits backfilling lowstand incised valleys, and is assigned to the transgressive systems tract (TST), bounded above and below by the transgressive surface of erosion (TSE) and the downlap surface (DLS), respectively.
2. A basinward thickening, subtly offlapping unit up to 70 m thick, contains moderate to low amplitude reflectors, which downlap onto older deposits and infill palaeotopography. This unit is interpreted as comprising mainly fine grained aggradational and mildly progradational marine sediments of the highstand systems tract (HST).
3. In some cases (basin cycles 25, 26, 27, 34, 35, 39, and 40), a basinward-thickening (up to 20 m thick), progradational wedge that sits basinward of the HST is preserved below the superjacent sequence boundary. Internal reflectors are low to high amplitude. This unit is interpreted as corresponding to rapid basinward progradation of the nearshore sediment wedge during periods of glacio-eustatic fall, or "forced regression". The unit is assigned to the regressive systems tract (RST; *sensu* Naish & Kamp 1997; Browne & Naish 2003).

Each sequence is bounded below by a sharp, planar, regionally extensive, discontinuity that exhibits erosional relief. These sequence boundaries truncate underlying RSTs and HSTs, and are overlain by TSTs. We interpret the boundaries as transgressive surfaces of erosion superposed on subaerial unconformities, and surmise that in most cases, the upper parts of sequences have been truncated by transgressive shoreface erosion. Systems tracts have not been identified for non-marine sequences corresponding to basin cycles 18 and 19 in the Lower Maxwell Formation. Our sequence stratigraphic interpretations are supported and constrained by correlation of individual systems tracts and surfaces from the subsurface into the coastal outcrop. These correlations are constrained where behind outcrop drill holes intersect the GNS Wanganui seismic line.

The seismic stratigraphic sequences can be grouped into three major packages separated by regional unconformities representing durations equivalent to one or more orbital cycles. The three sequence packages include: (1) basin cycles 12–20, (2) basin cycles 23–27, and (3) basin cycles 31–40. Sequences in the lower package are Nukumaruan in age, display local relief of up to several metres on their sequence boundaries, are comparatively thin, and do not thicken in a basinward direction. These sequences were not drilled on the GNS Wanganui seismic line, rather they were recovered c. 5 km along the coast from the north-west end of the seismic line by Ototoka-1 drill core. Correlation between the outcrop/drill core and the seismic line was achieved by extrapolation of sequence thicknesses in the borehole along the regional dip. Sequences in the middle package were not observed in coastal outcrop as they were accumulating in a basinward setting during a time of coeval erosion at the coast recorded by the unconformity beneath the Butlers Shell Conglomerate. The stratigraphic relationships are complex in this package as sequence bounding unconformities, which display significant channelled relief, progressively cut out older sequences from east to west along the seismic profile towards the position of the base of the Butlers Shell Conglomerate unconformity in the coastal outcrop. The basinward reduction in erosion at sequence boundaries, together with basinward thickening of sequences, suggest progressive increase in accommodation within the middle package south-east of a localised subaerial high. The sequence stratigraphic interpretation of the Kai-iwi-1 core together with the chronostratigraphic data described above has allowed the recognition of basin cylces 23–27 (MIS 54–45) (Fig. 8).

Seismic-borehole correlation

Although visual correlation of the outcrop stratigraphy down dip into the subsurface via sequence stratigraphic interpretation of the seismic data closely matched interpretations of the drill core stratigraphic records, a seismic well tie was undertaken for Castlecliff-1A (Fig. 7). Schlumberger's GeoQuest IESX software was used to develop a synthetic seismogram for Castlecliff-1A to enable the seismic reflection data to be frequency matched with the borehole and core data. The high resolution sonic and density logs were used directly to calculate seismic impedance, as the slow logging speed and high sample density resulted in very clean logs with little spiking. The sonic log alone was used for the depth-time conversion. A number of different wavelets were developed and tested, with the optimal wavelet of 32 ms being deterministically derived from the data. The wavelet was mixed phase, but this corresponded well to the combination of (near minimum phase) dynamite source and the non-phase preserving processing sequence (Melhuish 1994).

The amplitude of the synthetic seismogram corresponded closely with the amplitude variation of the seismic reflection data, with the strongest impedance contrasts occurring across siltstone-shellbed/sandstone contacts marked by sequence boundaries and downlap surfaces. This observation confirmed our ability to interpret the seismic reflection profile at systems tracts level, and subsurface core to outcrop correlation of the sequences.

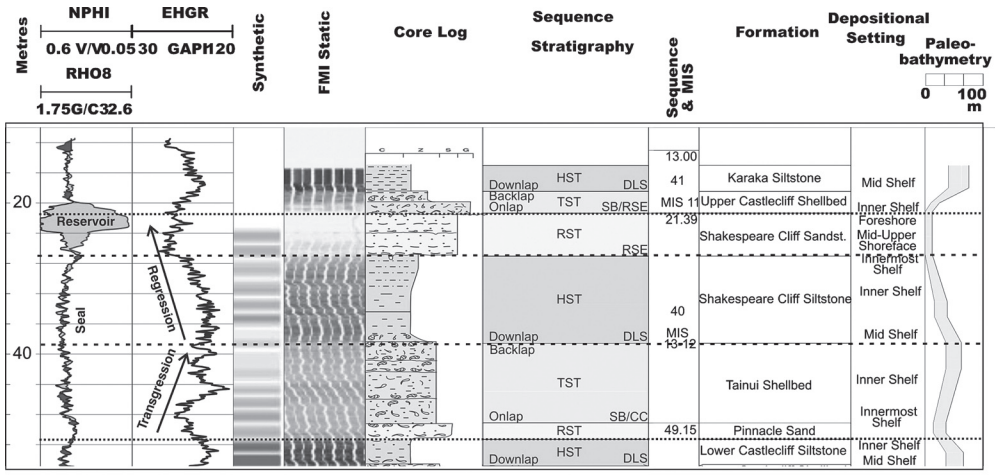

Fig. 15 Integrated well-log, image log, seismic, and core signatures of a representative high frequency depositional sequence, Castlecliff-1A.

DISCUSSION

Petroleum exploration significance

Over the last 20 years innovative new technologies, together with vastly improved computer-processing capabilities, have revolutionised the search for oil and gas. Consequently, producing basins and fields are becoming more intensely developed and geoscientists are requiring more accurate techniques for stratigraphic analysis. Many exploration companies are routinely acquiring high resolution seismic lines comprising 3D seismic surveys over fields, well image logs, and are coring more to quantify reservoir properties. In hydrocarbon producing regions, such as Taranaki Basin, with sufficient density of well control, the integration of well logs, cores, and seismic sequence stratigraphy can produce an "ultra" high resolution chronostratigraphic framework for subsurface correlation.

While Wanganui Basin is not recognised as a hydrocarbon-prospective province, the tightly constrained outcrop and subsurface seismic, core and well-log dataset presented in this paper serves as an excellent analogue, or training package, for understanding the stratigraphic signatures and 2D architecture of cyclical shallow-marine depositional systems. Similar such systems within the Eocene Kapuni Group (e.g., Mangahewa and Kaimiro formations) have been, and still are, the focus of intense exploration and production in Taranaki Basin.

Current interpretations of the broad scale depositional architecture of Wanganui Basin (Kamp et al. 2002) view the Early Pliocene-Pleistocene fill as a single 2nd order (5 Ma duration), northward prograding continental margin wedge, named the Rangitikei Megasequence. Our study samples the strongly progradational upper 500 m of the megasequence, which was deposited during the last 2 Ma, under conditions of reducing, and southwestward-migrating accommodation space. During this time substantial volumes of terrigenous sediment supplied to the basin from erosion of the Southern Alps and North Island ranges kept pace with the rate of subsidence maintaining a shallow-marine depositional setting. The resulting stratigraphic architecture has been strongly influenced by transgressions and regressions of the shoreline across the region in response to as many as 40 global glacio-eustatic sea-level fluctuations producing the progradational stacking of high-frequency (5th and 6th order) depositional sequences displayed in Fig. 14 and 15. Our integrated dataset shows that potential reservoir

facies, shallow-marine sandstones, are distributed regionally during transgressions, and in most cases preserved by widespread siltstone deposition at sea-level highstands. Ensuing regressive shoreline sandstone deposits may also be widespread, but are more commonly of lesser areal extent due to their partial removal, and in some cases complete removal, by the next phase of transgressive shoreface erosion. Though generally less widespread, they are typically less cemented and likely to have better reservoir potential than transgressive systems tracts in this basin. In a hydrocarbon prospective basin, an understanding of the distribution of reservoir facies and intervening seal rocks (siltstone facies) within sequences, together with the nature of the connectivity of sandstone facies between sequences, is a critical part of evaluating reservoir quality and production potential.

ACKNOWLEDGMENTS

Drillwell Exploration Ltd is thanked for expertise in managing drilling operations. Schlumberger Data Services Ltd, New Plymouth ran wireline and image logs. Erica Vye, Jeremy Mitchell, and Matt Patterson are thanked for drill site assistance and core logging. Don McFarlane is thanked for handling drilling contract tender process and providing on-site advice. Colin Gower, Wanganui District Council Water Services, is thanked for his assistance. This research was jointly funded by the Australian Research Council (Grant SIG A-39805139), New Zealand Foundation for Research, Science and Technology (CO5086 and CO5X0202), Natural Environmental Research Council, Schlumberger Data Services Ltd, and the Alfred-Wegener-Institute, Germany. John Westgate, University of Toronto is thanked for providing laboratory facilities for microprobe analysis of tephra. Sue Shaw is thanked for assistance with drafting. Referee reports by Lionel Carter and Alan Beu helped improve this paper.

REFERENCES

Abbott ST 1997. Foraminiferal paleobathymetry and mid-cycle architecture of mid-Pleistocene depositional sequences, Wanganui Basin, New Zealand. Palaios 12(3): 267–281.

Abbott ST, Carter RM 1994. The sequence architecture of mid-Pleistocene (c.1.1–0.4 Ma) cyclothems from New Zealand; facies development during a period of orbital control on sea-level cyclicity. Orbital forcing and cyclic sequences. Special Publication of the International Association of Sedimentologists 19: 367–394.

Abbott ST, Naish TR, Carter RM, Pillans BJ 2005. Sequence stratigraphy of the Nukumaruan Stratotype, (Pliocene-Pleistocene, c. 2.08–1.63 Ma), Wanganui Basin, Journal of the Royal Society of New Zealand 35: 123–150 (this issue).

Alloway BV, Pillans BJ, Sandhu AS, Westgate JA 1993. Revision of the marine chronology in the Wanganui Basin, New Zealand based on the isothermal plateau fission-track dating of tephra horizons. Sedimentary Geology 82(1–4): 299–310.

Alloway BV, Pillans BJ, Naish TR, Carter L, Westgate JA 2005. Onshore-offshore correlation of Pleistocene rhyolitic eruptions from New Zealand: implications for TVZ eruptive history and paleoenvironmental reconstruction. Quaternary Science Reviews: in press.

Anderton PW 1981. Structure and evolution of the South Wanganui Basin, New Zealand. New Zealand Journal of Geology and Geophysics 24: 39–63.

Barker A 2001. Magnetostratigraphy of Plio-Pleistocene drill cores from Wanganui Basin, New Zealand. Unpublished MSc thesis, University of Oxford. 56 p.

Beu AG, Edwards AR 1984. New Zealand Pleistocene and late Pliocene glacio-eustatic cycles. Third International Meeting on Pacific Neogene Stratigraphy 46(1–3). Pp. 119–142.

Beu AG, Alloway BV, Cooper RA, Crundwell MP, Kamp PJJ, Mildenhall DC, Naish TR, Scott GH, Wilson GS 2004. Chapter 13, Pliocene, Pleistocene, Holocene. In: Cooper RA ed 2004. The New Zealand geological timescale. Institute of Geological and Nuclear Sciences Monograph 22. 284 p.

Butler RF 1992. Paleomagnetism. Boston, Blackwell Scientific Publications.

Browne GH, Naish TR 2003. Facies development and sequence architecture of a late Quaternary fluvial-marine transition, Canterbury Plains and shelf, New Zealand; implications for forced regressive deposits. Sedimentary Geology 158(1–2): 57–86.

Browne GH, Slatt RM, King PR 2000. Contrasting styles of basin floor fan and slope fan deposition: Mount Messenger Formation, New Zealand. American Association of Petroleum Geologists Memoir 72, SEPM Special Publication 68: 143–152.

Carter L, Nelson CS, Neil HL, Froggatt PC 1995. Correlation, dispersal, and preservation of the Kawakawa Tephra and other late Quaternary tephra layers in the Southwest Pacific Ocean. New Zealand Journal of Geology and Geophysics 38(1): 29–46.

Carter L, Shane PAR, Alloway B, Hall IR, Harris SE, Westgate JA 2003. Demise of one volcanic zone and birth of another; a 12 m.y. marine record of major rhyolitic eruptions from New Zealand. Geology 31(6): 493–496.

Carter RM, Abbott ST, Naish TR 1999. Plio-Pleistocene cyclothems from Wanganui Basin, New Zealand; type locality for an astrochronologic time-scale, or template for recognizing ancient glacio-eustasy? Philosophical Transactions Royal Society. Mathematical, Physical and Engineering Sciences 357: 1861–1872.

Carter RM, Fulthorpe CS, Naish TR 1998. Sequence concepts at seismic and outcrop scale; the distinction between physical and conceptual stratigraphic surfaces. Sequence stratigraphy in the Plio-Pleistocene; an evaluation. Sedimentary Geology 122(1–4): 165–169.

Fleming CA 1953. The geology of the Wanganui Subdivision. Bulletin of the Geological Society of New Zealand 52. P. 362.

Kamp PJJ, McIntyre AP 1998. The stratigraphic architecture of late Pliocene (2.8–2.4 Ma) asymmetrical shelf sequences, western Wanganui Basin, New Zealand. Sequence stratigraphy in the Plio-Pleistocene; an evaluation. Sedimentary Geology 122(1–4): 53–67.

Kamp, PJJ, Vonk AJ, Bland KJ, Griffin AG, Hayton S, Hendy AJW, McIntyre AP, Naish TR, Nelson CS 2002: Megasequence architecture of Taranaki-Wanganui-King Country Basins and Neogene progradation of two continental margin wedges across western New Zealand. Proceedings of the 2002 New Zealand Petroleum Conference. Pp. 464–481.

King PR, Browne GH, Slatt RM 1994. Sequence architecture of exposed late Miocene basin floor fan and channel-levee complexes (Mount Messenger Formation), Taranaki Basin, New Zealand. Submarine fans and turbidite systems; sequence stratigraphy, reservoir architecture and production characteristics, Gulf of Mexico and International Society of Economic Paleontologists and Mineralogists. Gulf Coast Section 15: 177–192.

Kitamura A, Matsui H, Oda, M 2000. Constraints on the timing of systems tract development with respect to sixth-order (41ka) sea-level changes; an example from the Pleistocene Omma Formation, Sea of Japan. Sedimentary Geology 131(1–2): 67–76.

Kondo Y, Abbott ST, Kitamura A, Kamp PJJ, Naish TR, Kamataki T, Saul GS 1998. The relationship between shellbed type and sequence architecture; examples from Japan and New Zealand. Sedimentary Geology 122(1–4): 109–127.

Le Maitre RW 1984. A proposal by the IUGS subcommission on the systematics of igneous rocks for a chemical classification of volcanic rocks based on total alkai silica (TAS) diagram. Australian Journal of Earth Sciences 31: 243–255.

Melhuish A 1994. Acquisition and processing of seismic reflection data on the beach north of Wanganui, New Zealand. Institute of Geological and Nuclear Sciences Client Report 554 91K. 25 p.

Naish TR, Kamp PJJ 1997. Sequence stratigraphy of sixth-order (41 k.y.) Pliocene-Pleistocene cyclothems, Wanganui Basin, New Zealand; a case for the regressive systems tract. Geological Society of America Bulletin 109(8): 978–999.

Naish TR, Kamp PJJ, Alloway BV, Pillans BJ, Wilson GS, Westgate JA 1996. Integrated tephrochronology and magnetostratigraphy for cyclothemic marine strata, Wanganui Basin; implications for the Pliocene-Pleistocene boundary in New Zealand. Quaternary International 34–36: 29–48.

Naish TR, Abbott SA, Alloway BV, Beu AG, Carter RM, Edwards AR, Journeaux TD, Kamp PJJ, Pillans BJ, Saul G, Woolfe KJ 1998. Astronomical calibration of a Southern Hemisphere Plio-Pleistocene reference section, Wanganui Basin, New Zealand. Quaternary Science Reviews 17(8): 695–710.

Naish TR, Wheland F, Wilson, GS, Browne GH, Cook RA, Morgans HEG, Rosenberg M, King PR, Smale D, Nelson CS, Kamp PJJ, Ricketts B 2005. An integrated sequence stratigraphic, palaeoenvironmental, and chronostratigraphic analysis of the Tangahoe Formation, southern Taranaki coast, with implications for mid-Pliocene (c. 3.4–3.0 Ma) glacio-eustatic sea-level changes. Journal of the Royal Society of New Zealand 35: 151–196 (this issue).

Nelson CS, Froggatt P, Gosson P 1986. Nature, chemistry, and origin of late Cenozoic megascopic tephras in Leg 90 cores from the southwest Pacific. Initial reports of the Deep Sea Drilling Project 90 (Part 2). Pp. 1161–1173.

Niessen F, Jarrard RD, Bucker C 1998. Velocity and porosity of sediments from CRP-1 Drillhole, Ross Sea, Antarctica. Terra Antartica 5(3): 311–318.

Pillans BJ, Roberts AP, Wilson GS, Abbott ST, Alloway BV 1994. Magnetostratigraphic, lithostratigraphic and tephrostratigraphic constraints on lower and middle Pleistocene sea-level changes, Wanganui Basin, New Zealand. Earth and Planetary Science Letters 121(1–2): 81–98.

Pillans BJ, Alloway BV, Naish TR, Westgate JA, Abbott SA, Palmer A 2005. Silicic tephras in Pleistocene shallow-marine sediments of Wanganui Basin, New Zealand. Journal of the Royal Society of New Zealand 35: 43–90 (this issue).

Ravens J 1999. Globe claritas, seismic processing directory. Institute of Geological and Nuclear Sciences Technical Report 99/12. 307 p.

Saul G, Naish TR, Abbott ST, Carter RM 1999. Sedimentary cyclicity in the marine Pliocene-Pleistocene of the Wanganui Basin (New Zealand); sequence stratigraphic motifs characteristic of the past 2.5 m.y. Geological Society of America Bulletin 111(4): 524–537.

Shackleton NJ, Berger A, Peltier WA 1990. An alternative astronomical calibration of the lower Pleistocene timescale based on ODP Site 677. Transactions of the Royal Society of Edinburgh. Earth Sciences 81(4): 251–261.

Shane PAR, Black TM, Alloway BV, Westgate JA 1996. Early to middle Pleistocene tephrochronology of North Island, New Zealand; implications for volcanism, tectonism, and paleoenvironments. Geological Society of America Bulletin 108(8): 915–925.

Turner GM, Kamp PJJ 1990. Palaeomagnetic location of the Jaramillo Subchron and the Matuyama-Brunhes transition in the Castlecliffian stratotype section, Wanganui Basin, New Zealand. Earth and Planetary Science Letters 100(1–3): 42–50.